For lung histology, mice were sacrificed by CO_2 asphyxiation 48 h after the last OVA inhalation on day 16, and the lungs were infused with 10% (v/v) Formalin in PBS for fixation. The lung samples were sectioned, stained with H&E reagents, and examined for pathological changes under a light microscope at ×200. Numbers of infiltrated mononuclear cells in the perivascular and peribronchiolar regions were enumerated by direct counting of four different fields per slide as described previously (51).

Results

Phenotypic and functional characterization of aging mouse CD4$^+$ T cells

We initiated the analysis of T cells of aging C57BL/6 mice (8–12 mo) maintained under specific pathogen-free conditions by examining the expression of cell surface molecules on splenic CD4$^+$ T cells. Representative CD4/CD8 profiles for young and aging mice are shown in Fig. 1*A*. The yields of spleen cells were 112 ± 24 × 10^6 (n = 8) for young mice and 134 ± 34 × 10^6 (n = 8) for aging mice. The percentages of CD4$^+$ and CD8$^+$ T cells in the spleen were similar between young and aging mice, and the cell surface expression of TCR$\alpha\beta$ and CD3 on the splenic CD4$^+$ T cells was also similar (Fig. 1*B*). However, the numbers of CD25$^+$ cells, CD69$^+$ cells, and memory type (CD44^{high}) CD4$^+$ T cells in aging mice were higher than in young mice. The expression level of IL-4Rα on CD4$^+$ T cells was slightly higher in aging mice. As for T cell function, the anti-TCRβ mAb-induced proliferative responses of CD4$^+$ T cells were lower in aging mice (Fig. 1*C*). We examined the anti-TCR-induced cell division of CD4$^+$ T cells in Th1- or Th2-skewed differentiation cultures and found that CFSE-labeled naive CD4$^+$ T cells were stimulated by the anti-TCRβ mAb in the presence of IL-2 and IL-12 (Th1 culture conditions) or IL-2 and IL-4 (Th2 culture conditions). After 72 h of culture, the cells had divided three to four times in the case of both young and aging mouse T cells. The rate of cell division of aging mouse CD4$^+$ T cells was slightly impaired under either Th1- or Th2-skewed conditions (Fig. 1*D*). Similar results were obtained using CD4$^+$ T cells form BALB/c mice (data not shown). These results suggest that CD4$^+$ T cells from aging mice have a moderately decreased proliferative response to anti-TCR stimulation, a finding consistent with previous reports (17, 18).

In vitro Th1/Th2 cell differentiation of naive CD4$^+$ T cells from aging mice

Th1/Th2 cell differentiation of naive CD4$^+$ T cells from young and aging mice was examined using a well-established in vitro culture system (5). Naive CD4$^+$ T cells from aging OVA-specific TCR$\alpha\beta$ Tg (DO11.10 Tg) mice were sorted and stimulated with antigenic OVA peptide in the presence of young BALB/c APCs for 5 days. CD4$^+$ T cells from young DO11.10 Tg mice preferentially differentiated into IL-4-producing Th2 cells in an Ag dose-dependent fashion (Fig. 2, *left upper panels*). However, for aging mice, the generation of Th2 cells was decreased, and a significant increase in the number of IFN-γ-producing Th1 T cells was observed (Fig. 2, *left panels*). The levels of Th2 cell differentiation induced by a minimal dose of antigenic peptide (0.1 μM), and exogenous IL-4 was also decreased in old DO11.10 Tg T cell cultures (Fig. 2, *middle panels*). In contrast, the IL-12-dependent induction of Th1 cell differentiation remained intact (Fig. 2, *right panels*). These results suggest that the efficiency of Th2 cell differentiation is reduced in aging mice.

Anti-TCR-induced cytokine production profiles of splenic CD4$^+$ T cells from aging mice

Purified BALB/c CD4$^+$ T cells from young and aging mice were stimulated in vitro with immobilized anti-TCRβ mAb, and the level of cytokines in the culture supernatant was determined by ELISA (Fig. 3). The levels of IL-2 were not obviously decreased on day 2 but decreased on day 3. The production of IFN-γ in aging mouse CD4$^+$ T cell cultures was substantially increased on day 5 and day 7. In contrast, the levels of all Th2 cytokines, IL-4, IL-5, and IL-13, in aging mouse T cell cultures were decreased on days

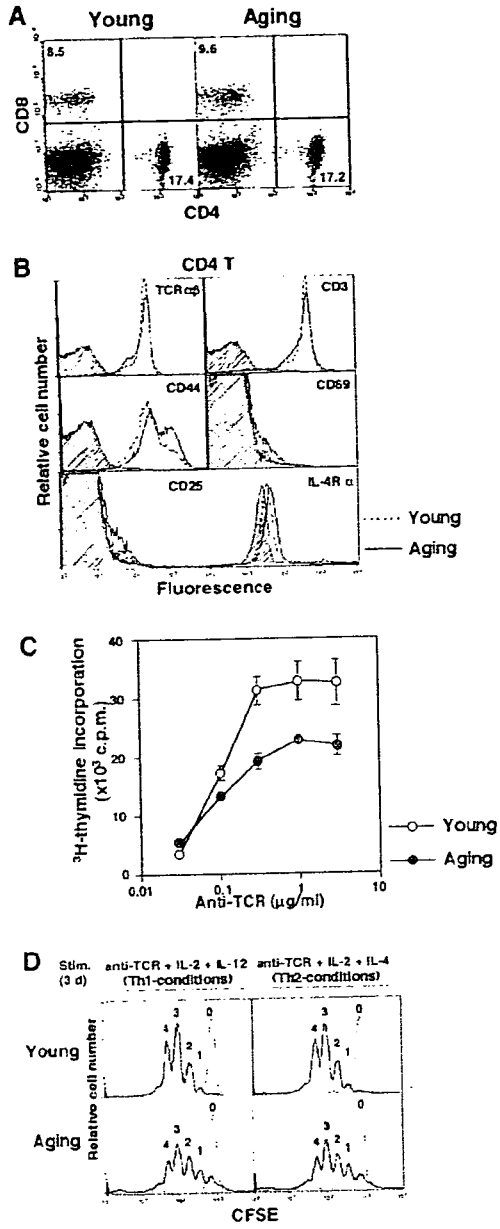

FIGURE 1. Phenotypic and functional characterization of aging mouse T cells. *A*, Representative CD4/CD8 profiles of splenocytes of young (6 wk old) and aging (9 mo old) C57BL/6 mice are shown. Percentages of cells present in each area are also shown. *B*, Each histogram depicts the expression of the indicated marker Ags on electronically gated splenic CD4$^+$ T cells from young (dotted lines) and aging (solid lines) mice. Background staining is shown as hatched areas. *C*, Splenic CD4$^+$ T cells from young (○) and aging (●) mice were stimulated with immobilized anti-TCRβ mAb. The mean [^{3}H]thymidine incorporation of each group is shown with SDs. *D*, Naive CD4$^+$ T cells were labeled with CFSE and stimulated with immobilized anti-TCRβ mAb under Th1- or Th2-skewed conditions. After 3 days of culture, the number of cell divisions (0 to 4) was assessed by flow cytometry.

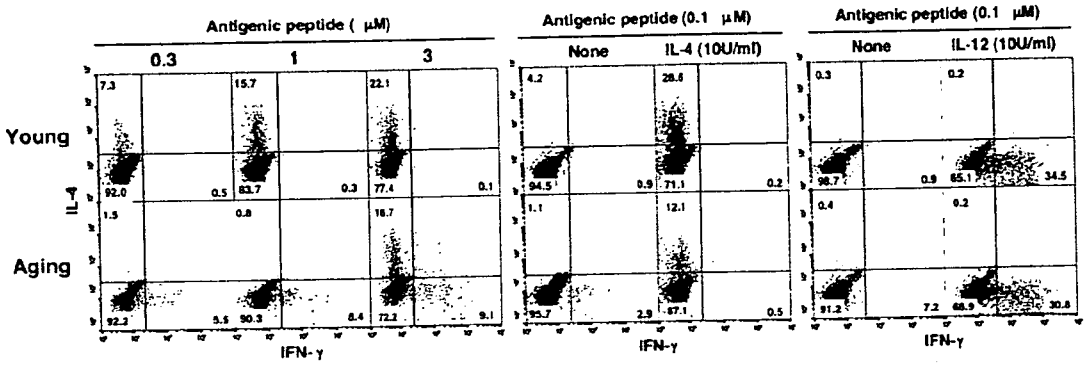

FIGURE 2. In vitro Th1/Th2 cell differentiation of naive CD4$^+$ T cells from aging mice. Naive (CD44^{low}) CD4$^+$ T cells purified by cell sorting from the spleens of aging OVA-specific TCR$\alpha\beta$ Tg (DO11.10 Tg) mice were stimulated with the indicated doses of antigenic peptide (OVA; 323–339) and irradiated young BALB/c APCs (*left panel*), a minimal dose of peptide (0.1 μM) and APCs in the presence of exogenous IL-4 (*middle panel*) or IL-12 and anti-IL-4 mAb (*right panel*) for 5 days. Intracellular staining profiles of IFN-γ and IL-4 are shown with percentages of cells in each area. The results are representative of five experiments.

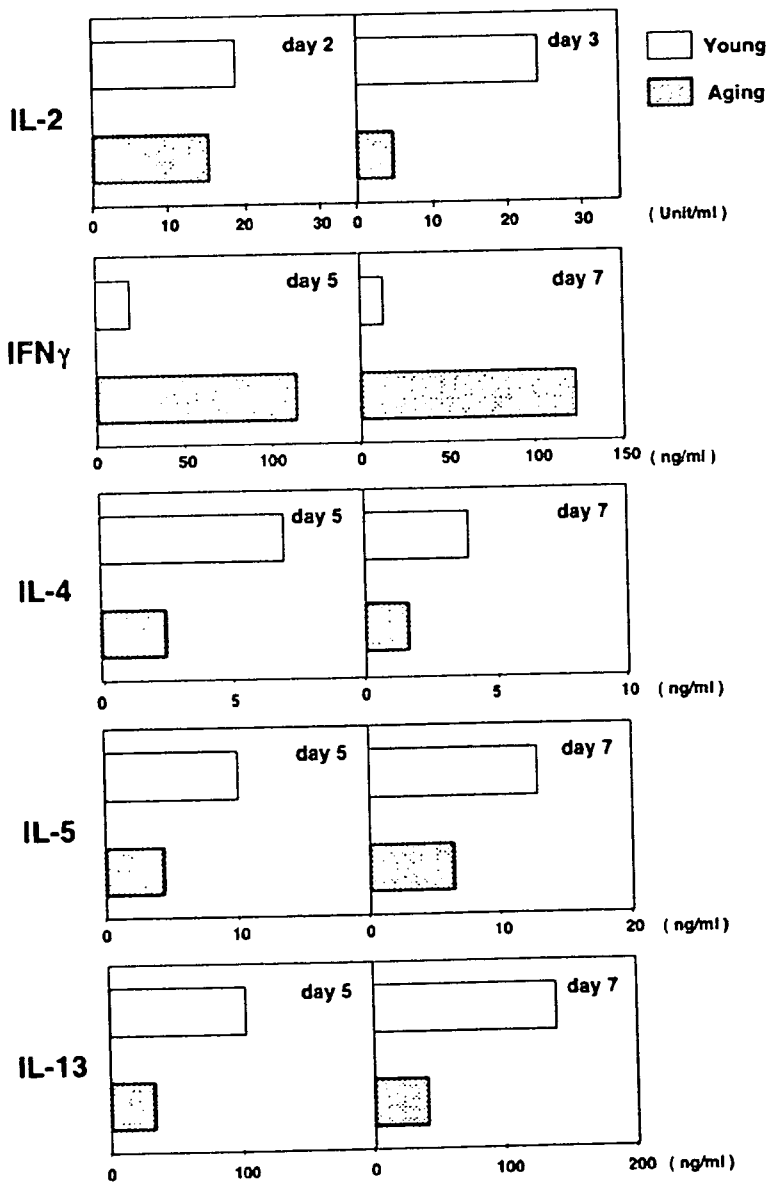

FIGURE 3. Decreased Th2 cytokine production in aging mouse CD4$^+$ T cells. Purified BALB/c splenic CD4$^+$ T cells were stimulated with immobilized anti-TCRβ mAb for 2 and 3 days (IL-2), or 5 and 7 days (IL-4, IL-5, IL-13, and IFN-γ). The concentration of cytokines in the culture supernatant was determined by ELISA. Three independent experiments were performed with similar results.

5 and 7. Similar cytokine production profiles were obtained in the anti-CD3 stimulation cultures (data not shown).

Th1/Th2-dependent Ab production in aging mice

Th2 cells play an important role in the stimulation of B cells to produce high levels of Ag-specific IgG1 and IgE in vivo, whereas the IgG2a isotype is a consequence of the generation of Th1 cells. Young and aging BALB/c mice were immunized with OVA-CFA, and the serum concentrations of total IgE, OVA-specific IgG1 and IgG2a were measured. As expected, the serum concentration of total IgE was significantly decreased in aging mice (Fig. 4, *left panel*). The serum concentration of IgG1 was significantly lower in aging mice (Fig. 4, *middle panel*), while Th1-dependent OVA-specific IgG2a levels were not decreased (Fig. 4, *right panel*). The production of Ag-specific IgE was not detected (data not shown). These results suggest that Th2-dependent Ab responses in vivo are decreased in aging mice preserving Th1 responses intact.

Signal transduction downstream of IL-4R in $CD4^+$ T cells from aging mice

To assess the activation of the IL-4R signaling pathway, freshly prepared $CD4^+$ T cells from young and aging mice were stimulated with IL-4, and then the tyrosine phosphorylation of STAT6 was examined. No significant differences in the magnitude or time course of phosphorylation of STAT6 were observed (Fig. 5*A*). Protein expression of STAT6 was comparable between young and old mice. Moreover, STAT6 phosphorylation induced by various doses of IL-4 was also comparable (Fig. 5*B*). Thus, the IL-4R signaling cascade appears to be intact in $CD4^+$ T cells from aging mice.

Signal transduction through TCR in $CD4^+$ T cells from aging mice

Next, we assessed the levels of signaling activation downstream of TCR. First, $[Ca^{2+}]_i$ mobilization in $CD4^+$ T cells was assessed after TCR cross-linking, and a slightly higher percentages of responding cells and slightly higher magnitude of the response were observed (Fig. 5*C*). Next, naive $CD4^+$ T cells from young and aging mice were stimulated with anti-TCR mAb, and the tyrosine phosphorylation of ERK1 and ERK2, reflecting MAPKK activation, was examined (Fig. 5*D*). Although the expression levels of ERK1 and ERK2 protein were comparable, the levels of phosphorylation of both ERK1 and ERK2 were reduced substantially in $CD4^+$ T cells from aging mice. The background phosphorylation was also slightly reduced (see time 0). These results suggest that the activation of the Ras-ERK MAPK cascade is impaired in aging mouse $CD4^+$ T cells.

Decreased GATA3 induction in $CD4^+$ T cells differentiated under Th2 culture conditions

Because the levels of GATA3 and JunB expression are reported to be critical for Th2 cell differentiation (11), we assessed the protein and mRNA expression levels of GATA3 and JunB in developing Th2 cells. Naive $CD4^+$ T cells from young and aging BALB/c mice were stimulated with anti-TCRβ mAb in the presence of IL-4 and anti-IL-12 mAb for 5 days, and the protein expression levels of GATA3, JunB, and tubulin-α (Fig. 6*A*), and the mRNA expression levels of GATA3 (Fig. 6*B*) were assessed. The levels of GATA3 protein were decreased substantially in aging mouse $CD4^+$ T cells, while the levels of JunB were unchanged. Regarding the GATA3 mRNA levels, the decrease was significant but less dramatic in aging mouse T cells. These results suggest that GATA3 induction is significantly impaired in developing Th2 cells of aging mice.

In an attempt to rescue the inefficient Th2 cell differentiation in aging mouse T cells, we introduced GATA3 by retrovirus infection into aging mouse developing Th2 cells on day 2 of Th1/Th2 cell differentiation culture, and the generation of Th1/Th2 cells was assessed on day 5 (Fig. 6*C*). Although not complete, a substantial rescue of Th2 cell generation was observed. These results suggest that the inefficient Th2 cell differentiation in aging mouse T cells is due, at least in part, to the decreased expression of GATA3.

Chromatin remodeling of the Th2 cytokine gene locus in $CD4^+$ T cells from aging mice

We reported that Th2 responses are highly dependent on the extent of activation of the Ras-ERK MAPK cascade (6, 48). The hyperacetylation of histones associated with the Th2 cytokine gene locus is dependent on the expression of GATA3 (43, 46). Activation of the ERK-MAPK cascade is required for GATA3-dependent histone H3 hyperacetylation of the Th2 cytokine gene locus (16). Consequently, we wished to examine the chromatin remodeling of the Th2 cytokine gene locus in $CD4^+$ T cells from aging mice. The acetylation levels of histones associated with the Th2 cytokine gene locus (IL-4 promoter, IL-5 promoter, and IL-13 promoter) were reduced significantly in Th2 cells from aging mice (Fig. 7, *A* and *B*). The acetylation of the CNS1 region was reduced slightly in aging mouse Th2 cells. Similarly, the methylation levels of histones associated with the Th2 cytokine gene locus (IL-4 promoter, IL-5 promoter, and IL-13 promoter) and CNS1 region were significantly reduced in Th2 cells from aging mice (Fig. 7, *A* and *C*). These results indicate that histone H3 hyperacetylation and methylation of the Th2 cytokine gene locus are significantly decreased in developing Th2 cells of aging mice.

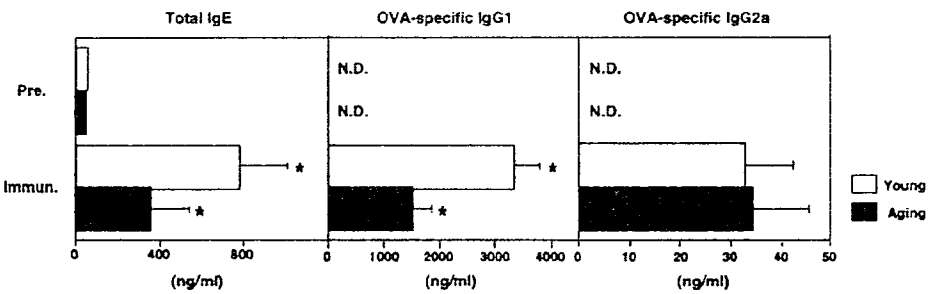

FIGURE 4. Th1/Th2-dependent immune responses in aging mice. Young (6 wk old) and aging (9 mo old) BALB/c mice (five mice per group) were immunized with OVA with CFA. Two weeks later, mean concentrations of total IgE and OVA-specific IgG1 and IgG2a Abs in the serum were determined. Data are shown with SEM. *, $p < 0.05$ by Student's t test. N.D., not detected.

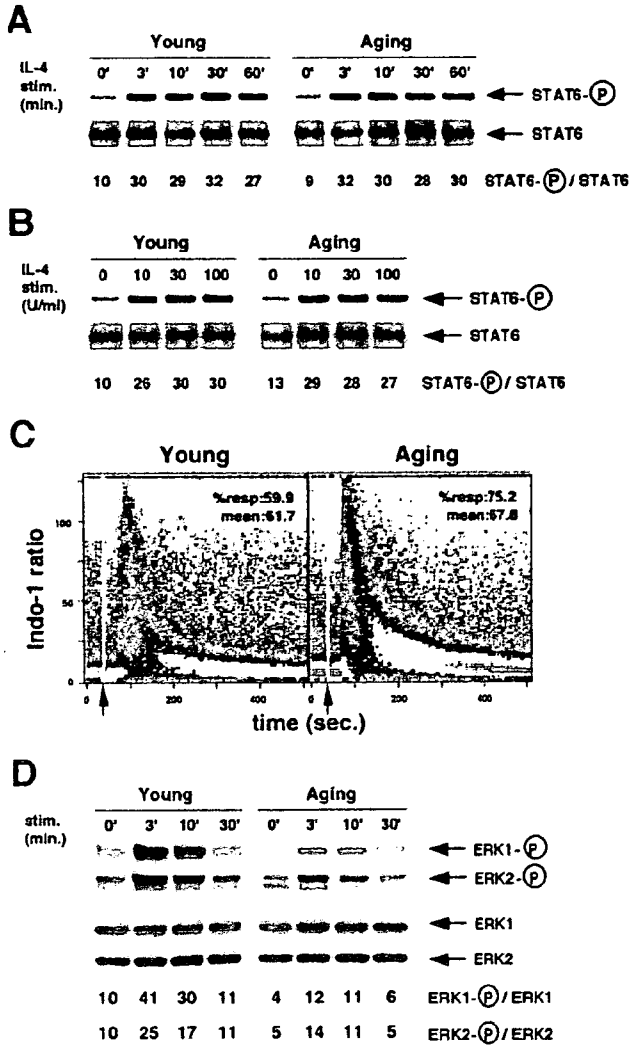

FIGURE 5. Signal transduction through TCR or IL-4R in $CD4^+$ T cells from young and aging mice. *A* and *B*, Naive $CD4^+$ T cells from young and aging mice were cultured for 2 days with immobilized anti-TCR mAb and IL-4, cultured without IL-4 for 8 h, and then the IL-4-induced phosphorylation on STAT6 (3–60 min with 100 U/ml IL-4 in *A*; 10 min with 10–100 U/ml IL-4 in *B*) was assessed by immunoprecipitation and immunoblotting with anti-phosphotyrosine mAb. The amount of STAT6 protein was also determined by reblotting the same membrane with specific mAbs. Arbitrary densitometric ratios (phospho-STAT6/STAT6) are shown under each band. Four independent experiments were done with similar results. *C*, Intracellular-free calcium ion levels after TCR-cross-linking (arrows) were measured by flow cytometric analysis of Indo-1-labeled naive $CD4^+$ T cells from young and aging mice. The mean ratio of violet to blue fluorescence of Indo-1 is plotted vs time following stimulation. Shown are data obtained by gating electronically on $CD4^+$ T cells. The percentages of responding cells and the mean response (ratio) of the responding cells are also shown. *D*, TCR-induced MAPKK activation in splenic $CD4^+$ T cells from aging mice. The phosphorylation status of ERK1 and ERK2 in splenic $CD4^+$ T cells was assessed 3–30 min after TCR cross-linking. After stimulation, the cells were lysed, and the lysates were subjected to immunoblotting with anti-phospho-ERK or anti-ERK Abs. Densitometric measurements of the phosphorylated bands (p44 for ERK1 and p42 for ERK2) are shown under each band in arbitrary units. Three independent experiments were done with similar results.

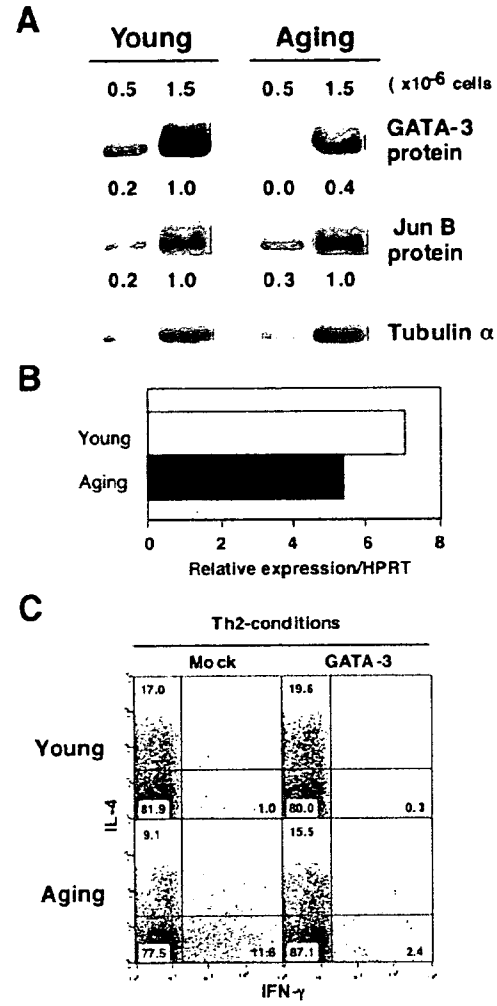

FIGURE 6. GATA3 expression and the effect of overexpression of GATA3 in developing Th2 cells from aging mice. *A*, GATA3 and JunB protein expression in developing Th2 cells. Naive $CD4^+$ T cells from BALB/c mice were stimulated with anti-TCRβ mAb in the presence of IL-4 and anti-IL-12 mAb for 5 days, and total nuclear extracts were analyzed by immunoblotting with anti-GATA3 mAb, anti-JunB mAb, or anti-tubulin-α mAb. Three independent experiments were performed; representative results are shown. Arbitrary densitometric units normalized to tubulin-α are shown under each band. *B*, GATA3 mRNA expression in young and aging developing Th2 cells. Th2 cells prepared as in *A* were subjected to quantitative RT-PCR analysis. *C*, Naive $CD4^+$ T cells from BALB/c mice were stimulated with anti-TCRβ mAb in the presence of IL-4 and anti-IL-12 mAb for 2 days and then infected with a mock or GATA3-containing retrovirus vector. Th1/Th2 cell differentiation was assessed on day 5.

Decreased OVA-induced eosinophilic infiltration in BAL fluid and airway inflammation in aging mice

Next, we examined the effect of aging on Th2-dependent immune responses in vivo. Young and aging BALB/c mice were immunized twice with OVA-alum, and 2 wk later, exposed to inhaled OVA as described in *Materials and Methods*. BAL fluid was harvested and examined for infiltrating leukocytes (Fig. 8, *A* and B). Eosinophils, lymphocytes, neutrophils, and macrophages were determined based on morphological criteria, and the absolute numbers and percentages of each cell type were determined. A substantial decrease in the absolute numbers (Fig. 8*A*) and percentages

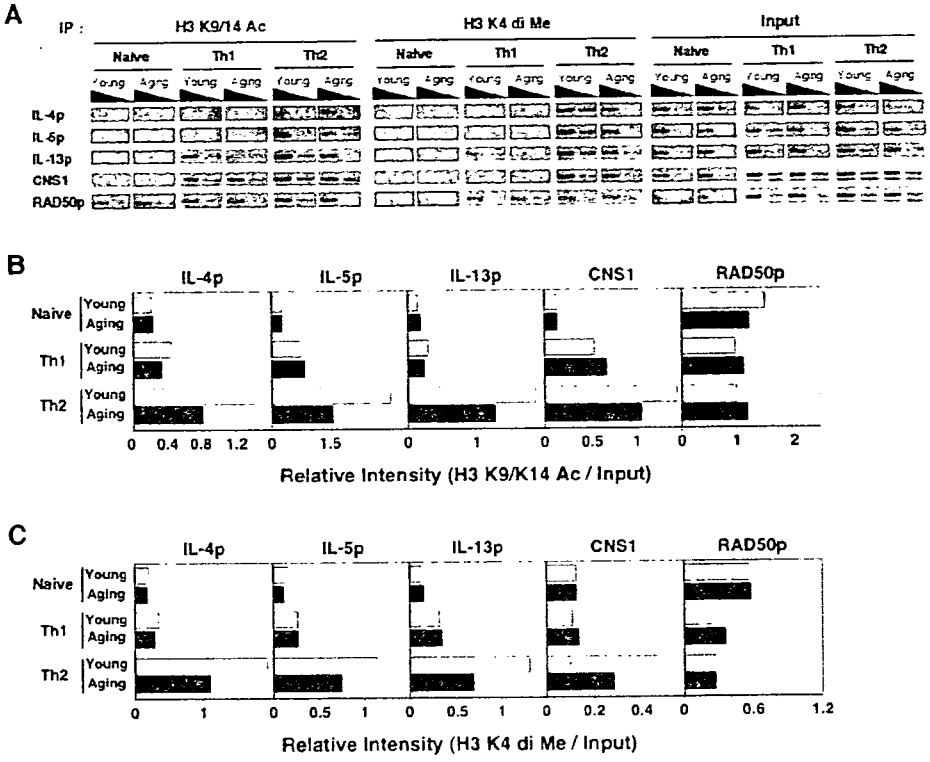

FIGURE 7. Histone modification of the Th2-cytokine locus in developing Th2 cells from aging mice. *A*, Acetylation and methylation status of histones associated with the Th2 cytokine gene locus. Freshly prepared naive splenic $CD4^+$ T cells were stimulated under Th1 or Th2 conditions for 5 days. The acetylation status and methylation status of histone H3 in nucleosomes associated with the indicated regions was assessed by ChIP assay. An anti-acetylated histone H3 (K9 and K14) Ab and an anti-histone H3 di-methyl K4 antiserum were used. *B*, The relative intensity of histone hyperacetylation (Ac-H3/input) in each group is shown in *A*. *C*, The relative intensity of histone dimethylation (diMe-H3/input) in each group is shown in *A*. Representative results of three independent experiments are shown.

(Fig. 8*B*) of eosinophils was observed in aging mice. The infiltration of macrophages was increased in aging mice, and the number of total infiltrating cells was decreased in aging mice. These results indicate that OVA-induced eosinophilic infiltration in the BAL fluid is decreased in aging mice.

Concurrently, histological changes in the lungs of young and aging mice were evaluated by HE staining (Fig. 8*C*). The absolute numbers and percentages of each cell type are shown (Fig. 8, *D* and *E*). The numbers of total infiltrating cells were indistinguishable between young and aging mice, although a slight decrease in the absolute number, and a slight, but significant, decrease in the percentage of eosinophils were observed. No apparent difference in the numbers of lymphocytes, neutrophils or macrophages was observed.

Discussion

In the present study, we used young adult (4–6 wk old) and aging (8–12 mo old) mice, to demonstrate that the levels of Th2 cell differentiation and Th2-dependent allergic airway inflammation are attenuated in aging mice. In addition, we found several molecular defects in aging mouse $CD4^+$ T cells, i.e., limited activation of the ERK/MAPK cascade, decreased expression of GATA3 and impaired chromatin remodeling of the Th2 cytokine gene locus. Because 8- to 12-wk-old mice can be considered to be in the early stages of aging, the processes affected would be the most sensitive among various age-related alterations in T cells.

Impaired Th2 cell differentiation in aging mouse $CD4^+$ T cell cultures was not restored by the addition of excess amounts of exogenous IL-4 (10 U/ml; Fig. 2, *middle panel*). In addition, our in vitro cultures contained sufficient amounts of exogenous IL-2 (30 U/ml). The production of all Th2 cytokines (IL-4, IL-5, and IL-13) was decreased in aging mouse $CD4^+$ T cells (Fig. 3). Thus, the defect in Th2 cell differentiation appears to be due to intrinsic alterations and not simply a secondary consequence of the imbalance in the production of IL-2, IL-4, or IFN-γ by aging mouse $CD4^+$ T cells in culture. Our observations are consistent with the results reported by H. al-Rayes et al. (52) that IL-4 production is diminished in aged human PBL.

In our previous reports, we showed that Th2 cell differentiation and Th2-dependent airway inflammation are highly dependent on the TCR-mediated activation of the Ras-ERK MAPK cascade (6, 48). In the present study, we detected significantly reduced activation of the Ras/MAPK cascade in aging mouse $CD4^+$ T cells (Fig. 5*D*). Thus, the impaired Th2 cell differentiation in old mice appears to be due to the decreased TCR-mediated activation of the Ras/MAPK signaling pathway.

As for Th1 cell differentiation, we observed no detectable decrease in IL-12-induced Th1 cell generation in vitro (Fig. 2, *right panels*), suggesting that the efficiency in Th1 cell differentiation is less affected by aging. We detected significant numbers of IFN-γ producing cells in aging naive $CD4^+$ T cell cultures when exogenous IL-4 was not included in the culture (Fig. 2, *left panels*). In addition, we detected increased production of IFN-γ by ELISA (Fig. 3). These results suggest that some shift from Th2 to Th1 cell differentiation occurs in aging mouse $CD4^+$ T cell cultures. We previously reported a dramatic shift from Th2 to Th1 cell differentiation in dominant negative Ras Tg mice (6). Therefore, these results also support the notion that the impaired Th2 cell differentiation in aging mice is due to the decreased TCR-mediated activation of the Ras/MAPK signaling pathway.

The expression levels of the GATA3 protein are critical for chromatin remodeling (46) and the maintenance of remodeled chromatin at the Th2 cytokine gene locus (14). In addition, we have recently demonstrated that the activation of the Ras-ERK MAPK cascade controls the stability of the GATA3 protein through the inhibition of ubiquitin-dependent degradation (16). The results presented in this report suggest that GATA3-dependent

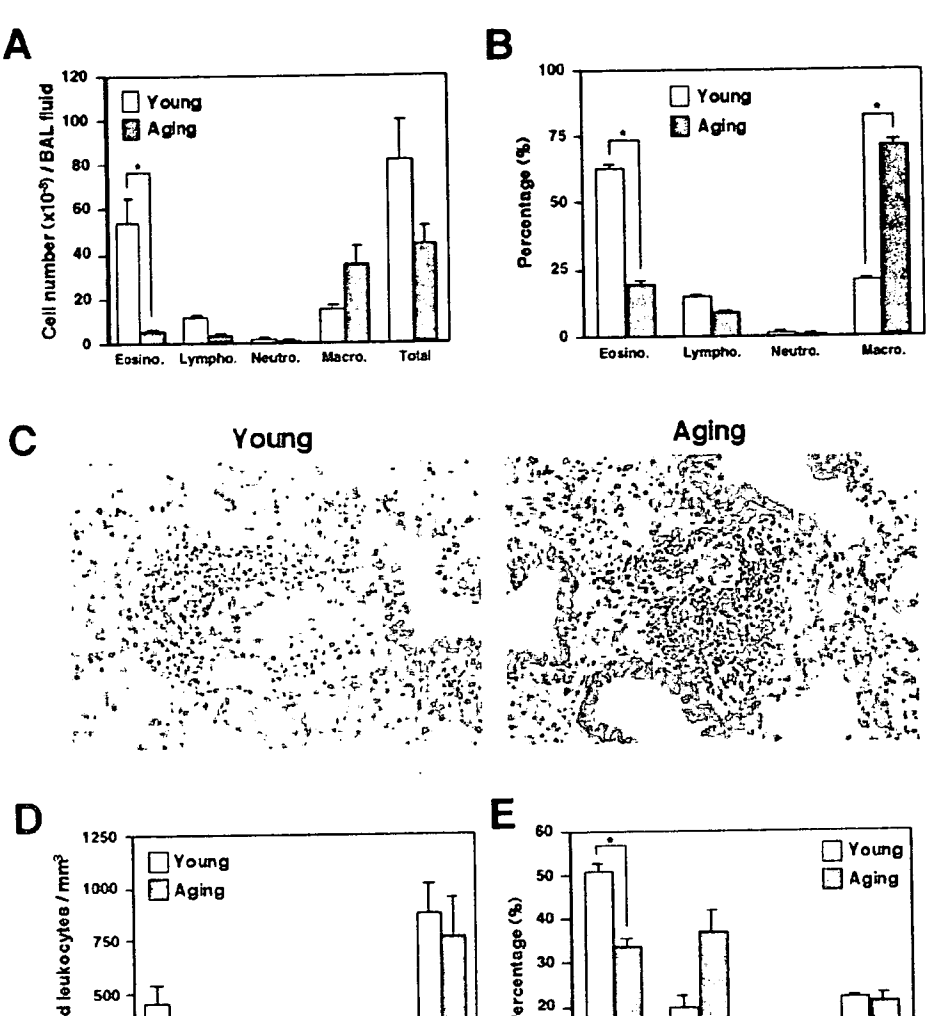

FIGURE 8. OVA-induced eosinophilic infiltration in BAL fluid and airway inflammation in old mice. The absolute cell number (*A*) and percentage (*B*) of eosinophils (Eosino.), lymphocytes (Lympho.), neutrophils (Neutro.), and macrophages (Macro.) in BAL fluid are shown with SDs. Three young (6 wk-old) and three aging (9 mo-old) BALB/c mice were used in this experiment. Data include absolute cell number, percentage of cells, total cell number per milliliter, and the volume of BAL fluid recovered. *, $p < 0.01$ and other p values >0.05 by Student's t test. *C*, OVA immunization and inhalation of OVA aerosol were done as in *A*. The lungs were fixed and stained with H&E, ×200. Sections shown are representative of 10 lung sections/mouse from three mice in each group. The cell number (*D*) and percentage (*E*) of infiltrated eosinophils (Eosino.), lymphocytes (Lympho.), neutrophils (Neutro.), and macrophages (Macro.) in the perivascular and peribronchiolar regions are shown with SDs. Three young (6 wk old) and three aging (9 mo old) BALB/c mice were used in this experiment. *, $p < 0.01$ and other p values >0.05 by Student's t test.

chromatin remodeling of the Th2 cytokine gene locus is significantly reduced in aging mouse $CD4^+$ T cells (Fig. 7). The expression levels of JunB (Fig. 6A) and the activation of NF-κB were comparable between young and aging mouse $CD4^+$ T cells (A. Hasegawa and T. Nakayama, unpublished observation). From these results, we conclude that the impaired chromatin remodeling of the Th2 cytokine gene locus in aging mice is due, at least in part, to the decreased expression of the GATA3 protein in developing Th2 cells.

Although it remains unclear why the activation of the Ras-ERK MAPK cascade is affected selectively during aging, this pathway may determine the characters of various T cell responses. In anergic CD4 T cells impaired activation of the Ras-ERK MAPK cascade has been reported (53, 54).

How allergic inflammation, such as allergic asthma is modulated by aging has not been reported. We show in the present study that the severity of Th2-dependent allergic airway inflammation is decreased in aging mice (Fig. 7). This appears to be due to the decreased Th2 cell differentiation in aging mice. Although there is as yet no clear evidence in humans, the data would suggest that the first onset of allergic asthma should occur less frequently in aged human beings. The confirmation of this hypothesis must await a comprehensive investigation in humans.

In summary, this study provides the first evidence that a chromatin-remodeling event in T cells, i.e., chromatin remodeling of the Th2 cytokine gene locus in developing Th2 cells, is compromised during aging. Moreover, we demonstrate attenuated Th2-dependent allergic airway inflammation in aging mice, which may reflect the nature of allergic diseases in aged humans.

Acknowledgments

We thank Kaoru Sugaya for excellent technical assistance.

Disclosures

The authors have no financial conflict of interest.

References

1. Mosmann, T. R., and R. L. Coffman. 1989. Th1 and Th2 cells: different patterns of lymphokine secretion lead to different functional properties. *Annu. Rev. Immunol.* 7: 145–173.
2. Abbas, A. K., K. M. Murphy, and A. Sher. 1996. Functional diversity of helper T lymphocytes. *Nature* 383: 787–793.
3. Constant, S. L., and K. Bottomly. 1997. Induction of Th1 and Th2 $CD4^+$ T cell responses: the alternative approaches. *Annu. Rev. Immunol.* 15: 297–322.
4. O'Garra, A. 1998. Cytokines induce the development of functionally heterogeneous T helper cell subsets. *Immunity* 8: 275–283.
5. Yamashita, M., K. Hashimoto, M. Kimura, M. Kubo, T. Tada, and T. Nakayama. 1998. Requirement for $p56^{lck}$ tyrosine kinase activation in Th subset differentiation. *Int. Immunol.* 10: 577–591.

6. Yamashita, M., M. Kimura, M. Kubo, C. Shimizu, T. Tada, R. M. Perlmutter, and T. Nakayama. 1999. T cell antigen receptor-mediated activation of the Ras/mitogen-activated protein kinase pathway controls interleukin 4 receptor function and type-2 helper T cell differentiation. *Proc. Natl. Acad. Sci. USA* 96: 1024–1029.
7. Yamashita, M., M. Katsumata, M. Iwashima, M. Kimura, C. Shimizu, T. Kamata, T. Shin, N. Seki, S. Suzuki, M. Taniguchi, and T. Nakayama. 2000. T cell receptor-induced calcineurin activation regulates T helper type 2 cell development by modifying the interleukin 4 receptor signaling complex. *J. Exp. Med.* 191: 1869–1879.
8. Grogan, J. L., and R. M. Locksley. 2002. T helper cell differentiation: on again, off again. *Curr. Opin. Immunol.* 14: 366–372.
9. Murphy, K. M., and S. L. Reiner. 2002. The lineage decisions of helper T cells. *Nat. Rev. Immunol.* 2: 933–944.
10. Zhang, D. H., L. Cohn, P. Ray, K. Bottomly, and A. Ray. 1997. Transcription factor GATA-3 is differentially expressed in murine Th1 and Th2 cells and controls Th2-specific expression of the interleukin-5 gene. *J. Biol. Chem.* 272: 21597–21603.
11. Zheng, W., and R. A. Flavell. 1997. The transcription factor GATA-3 is necessary and sufficient for Th2 cytokine gene expression in CD4 T cells. *Cell* 89: 587–596.
12. Ouyang, W., S. H. Ranganath, K. Weindel, D. Bhattacharya, T. L. Murphy, W. C. Sha, and K. M. Murphy. 1998. Inhibition of Th1 development mediated by GATA-3 through an IL-4-independent mechanism. *Immunity* 9: 745–755.
13. Lee, H. J., N. Takemoto, H. Kurata, Y. Kamogawa, S. Miyatake, A. O'Garra, and N. Arai. 2000. GATA-3 induces T helper cell type 2 (Th2) cytokine expression and chromatin remodeling in committed Th1 cells. *J. Exp. Med.* 192: 105–115.
14. Yamashita, M., M. Ukai-Tadenuma, T. Miyamoto, K. Sugaya, H. Hosokawa, A. Hasegawa, M. Kimura, M. Taniguchi, J. DeGregori, and T. Nakayama. 2004. Essential role of GATA3 for the maintenance of type 2 helper T (Th2) cytokine production and chromatin remodeling at the Th2 cytokine gene loci. *J. Biol. Chem.* 279: 26983–26990.
15. Pai, S. Y., M. L. Truitt, and I. C. Ho. 2004. GATA-3 deficiency abrogates the development and maintenance of T helper type 2 cells. *Proc. Natl. Acad. Sci. USA* 101: 1993–1998.
16. Yamashita, M., R. Shinnakasu, H. Asou, M. Kimura, A. Hasegawa, K. Hashimoto, N. Hatano, M. Ogata, and T. Nakayama. 2005. Ras-ERK MAPK cascade regulates GATA3 stability and Th2 differentiation through ubiquitin-proteasome pathway. *J. Biol. Chem.* 280: 29409–29419.
17. Miller, R. A. 1996. The aging immune system: primer and prospectus. *Science* 273: 70–74.
18. Globerson, A., and R. B. Effros. 2000. Ageing of lymphocytes and lymphocytes in the aged. *Immunol. Today* 21: 515–521.
19. Webster, R. G. 2000. Immunity to influenza in the elderly. *Vaccine* 18: 1686–1689.
20. Miller, R. A. 2000. Effect of aging on T lymphocyte activation. *Vaccine* 18: 1654–1660.
21. Chakravarti, B., and G. N. Abraham. 1999. Aging and T cell-mediated immunity. *Mech. Ageing Dev.* 108: 183–206.
22. Haynes, L., S. M. Eaton, E. M. Burns, T. D. Randall, and S. L. Swain. 2005. Newly generated CD4 T cells in aged animals do not exhibit age-related defects in response to antigen. *J. Exp. Med.* 201: 845–851.
23. Linton, P. J., L. Haynes, L. Tsui, X. Zhang, and S. Swain. 1997. From naive to effector: alterations with aging. *Immunol. Rev.* 160: 9–18.
24. Gillis, S., R. Kozak, M. Durante, and M. E. Weksler. 1981. Immunological studies of aging: decreased production of and response to T cell growth factor by lymphocytes from aged humans. *J. Clin. Invest.* 67: 937–942.
25. Engwerda, C. R., B. S. Handwerger, and B. S. Fox. 1996. An age-related decrease in rescue from T cell death following costimulation mediated by CD28. *Cell Immunol.* 170: 141–148.
26. Ginaldi, L., M. De Martinis, A. D'Ostilio, L. Marini, M. F. Loreto, M. P. Corsi, and D. Quaglino. 2000. Cell proliferation and apoptosis in the immune system in the elderly. *Immunol. Res.* 21: 31–38.
27. Li, M., R. Walter, C. Torres, and F. Sierra. 2000. Impaired signal transduction in mitogen activated rat splenic lymphocytes during aging. *Mech. Ageing Dev.* 113: 85–99.
28. Damjanovich, S., R. Gaspar, Jr., L. Bene, A. Jenei, and L. Matyus. 2003. Signal transduction in T lymphocytes and aging. *Exp. Gerontol.* 38: 231–236.
29. Garcia, G. G., and R. A. Miller. 1998. Increased Zap-70 association with CD3ζ in CD4 T cells from old mice. *Cell. Immunol.* 190: 91–100.
30. Miller, R. A. 1997. Age-related changes in T cell surface markers: a longitudinal analysis in genetically heterogeneous mice. *Mech. Ageing Dev.* 96: 181–196.
31. Cossarizza, A., C. Ortolani, R. Paganelli, D. Barbieri, D. Monti, P. Sansoni, U. Fagiolo, G. Castellani, F. Bersani, M. Londei, and C. Franceschi. 1996. CD45 isoforms expression on $CD4^+$ and $CD8^+$ T cells throughout life, from newborns to centenarians: implications for T cell memory. *Mech. Ageing Dev.* 86: 173–195.
32. Bandres, E., J. Merino, B. Vazquez, S. Inoges, C. Moreno, M. L. Subira, and A. Sanchez-Ibarrola. 2000. The increase of IFN-γ production through aging correlates with the expanded $CD8^{+high}CD28^-D57^+$ subpopulation. *Clin. Immunol.* 96: 230–235.
33. Sakata-Kaneko, S., Y. Wakatsuki, Y. Matsunaga, T. Usui, and T. Kita. 2000. Altered Th1/Th2 commitment in human $CD4^+$ T cells with ageing. *Clin. Exp. Immunol.* 120: 267–273.
34. Poynter, M. E., and R. A. Daynes. 1999. Age-associated alterations in splenic iNOS regulation: influence of constitutively expressed IFN-γ and correction following supplementation with PPARα activators or vitamin E. *Cell. Immunol.* 195: 127–136.
35. Karanfilov, C. I., B. Liu, C. C. Fox, R. R. Lakshmanan, and R. L. Whisler. 1999. Age-related defects in Th1 and Th2 cytokine production by human T cells can be dissociated from altered frequencies of $CD45RA^+$ and $CD45RO^+$ T cell subsets. *Mech. Ageing Dev.* 109: 97–112.
36. Mbawuike, I. N., C. L. Acuna, K. C. Walz, R. L. Atmar, S. B. Greenberg, and R. B. Couch. 1997. Cytokines and impaired $CD8^+$ CTL activity among elderly persons and the enhancing effect of IL-12. *Mech. Ageing Dev.* 94: 25–39.
37. Rink, L., I. Cakman, and H. Kirchner. 1998. Altered cytokine production in the elderly. *Mech. Ageing Dev.* 102: 199–209.
38. Ernst, D. N., M. V. Hobbs, B. E. Torbett, A. L. Glasebrook, M. A. Rehse, K. Bottomly, K. Hayakawa, R. R. Hardy, and W. O. Weigle. 1990. Differences in the expression profiles of CD45RB, Pgp-1, and 3G11 membrane antigens and in the patterns of lymphokine secretion by splenic $CD4^+$ T cells from young and aged mice. *J. Immunol.* 145: 1295–1302.
39. Kubo, M., and B. Cinader. 1990. Polymorphism of age-related changes in interleukin (IL) production: differential changes of T helper subpopulations, synthesizing IL 2, IL 3 and IL 4. *Eur. J. Immunol.* 20: 1289–1296.
40. Murphy, K. M., A. B. Heimberger, and D. Y. Loh. 1990. Induction by antigen of intrathymic apoptosis of $CD4^+CD8^+TCR^{low}$ thymocytes in vivo. *Science* 250: 1720–1723.
41. Nakayama, T., C. H. June, T. I. Munitz, M. Sheard, S. A. McCarthy, S. O. Sharrow, L. E. Samelson, and A. Singer. 1990. Inhibition of T cell receptor expression and function in immature $CD4^+CD8^+$ cells by CD4. *Science* 249: 1558–1561.
42. Kimura, M., Y. Koseki, M. Yamashita, N. Watanabe, C. Shimizu, T. Katsumoto, T. Kitamura, M. Taniguchi, H. Koseki, and T. Nakayama. 2001. Regulation of Th2 cell differentiation by mel-18, a mammalian polycomb group gene. *Immunity* 15: 275–287.
43. Inami, M., M. Yamashita, Y. Tenda, A. Hasegawa, M. Kimura, K. Hashimoto, N. Seki, M. Taniguchi, and T. Nakayama. 2004. CD28 costimulation controls histone hyperacetylation of the interleukin 5 gene locus in developing Th2 cells. *J. Biol. Chem.* 279: 23123–23133.
44. Kimura, M. Y., H. Hosokawa, M. Yamashita, A. Hasegawa, C. Iwamura, H. Watarai, M. Taniguchi, T. Takagi, S. Ishii, and T. Nakayama. 2005. Regulation of T helper type 2 cell differentiation by murine Schnurri-2. *J. Exp. Med.* 201: 397–408.
45. Omori, M., M. Yamashita, M. Inami, M. Ukai-Tadenuma, M. Kimura, Y. Nigo, H. Hosokawa, A. Hasegawa, M. Taniguchi, and T. Nakayama. 2003. CD8 T cell-specific down-regulation of histone hyperacetylation and gene activation of the IL-4 gene locus by ROG, repressor of GATA. *Immunity* 19: 281–294.
46. Yamashita, M., M. Ukai-Tadenuma, M. Kimura, M. Omori, M. Inami, M. Taniguchi, and T. Nakayama. 2002. Identification of a conserved GATA3 response element upstream proximal from the interleukin-13 gene locus. *J. Biol. Chem.* 277: 42399–42408.
47. Yamashita, M., R. Shinnakasu, Y. Nigo, M. Kimura, A. Hasegawa, M. Taniguchi, and T. Nakayama. 2004. Interleukin (IL)-4-independent maintenance of histone modification of the IL-4 gene loci in memory Th2 cells. *J. Biol. Chem.* 279: 39454–39464.
48. Shibata, Y., T. Kamata, M. Kimura, M. Yamashita, C. R. Wang, K. Murata, M. Miyazaki, M. Taniguchi, N. Watanabe, and T. Nakayama. 2002. Ras activation in T cells determines the development of antigen-induced airway hyperresponsiveness and eosinophilic inflammation. *J. Immunol.* 169: 2134–2140.
49. Hansen, G., G. Berry, R. H. DeKruyff, and D. T. Umetsu. 1999. Allergen-specific Th1 cells fail to counterbalance Th2 cell-induced airway hyperreactivity but cause severe airway inflammation. *J. Clin. Invest.* 103: 175–183.
50. Foster, P. S., S. P. Hogan, A. J. Ramsay, K. I. Matthaei, and I. G. Young. 1996. Interleukin 5 deficiency abolishes eosinophilia, airways hyperreactivity, and lung damage in a mouse asthma model. *J. Exp. Med.* 183: 195–201.
51. Kamata, T., M. Yamashita, M. Kimura, K. Murata, M. Inami, C. Shimizu, K. Sugaya, C. R. Wang, M. Taniguchi, and T. Nakayama. 2003. *src* homology 2 domain-containing tyrosine phosphatase SHP-1 controls the development of allergic airway inflammation. *J. Clin. Invest.* 111: 109–119.
52. al-Rayes, H., W. Pachas, N. Mirza, D. J. Ahern, R. S. Geha, and D. Vercelli. 1992. IgE regulation and lymphokine patterns in aging humans. *J. Allergy Clin. Immunol.* 90: 630–636.
53. Li, W., C. D. Whaley, A. Mondino, and D. L. Mueller. 1996. Blocked signal transduction to the ERK and JNK protein kinases in anergic $CD4^+$ T cells. *Science* 271: 1272–1276.
54. Fields, P. E., T. F. Gajewski, and F. W. Fitch. 1996. Blocked Ras activation in anergic $CD4^+$ T cells. *Science* 271: 1276–1278.

Lentivirus vectors expressing short hairpin RNAs against the *U3*-overlapping region of HIV *nef* inhibit HIV replication and infectivity in primary macrophages

Takuya Yamamoto, Hiroyuki Miyoshi, Norio Yamamoto, Naoki Yamamoto, Jun-ichiro Inoue, and Yasuko Tsunetsugu-Yokota

Although successful attempts to inhibit HIV-1 replication in T cells using RNAi have been reported, the effect of HIV-specific RNAi on macrophages is not well known. Macrophages are key targets for anti–HIV-1 therapy because they are able to survive long after the initial infection with HIV and can spread the virus to T cells. In this study, we identified a putative RNAi target of HIV, consisting of the portion of the *nef* gene overlapping the U3 region (Nef366), and generated a lentivirus-based short hairpin RNA (shRNA) expression vector (Lenti shNef366). We show that Lenti shNef366 inhibits (1) HIV-1 replication in a monocytic cell line and in primary monocyte-derived macrophages (MDMs), (2) reactivation of latent HIV-1 infection, and (3) the production of secondary HIV-1 from MDMs harboring a genomic copy of Nef366. Moreover, we found that the up-regulated production of macrophage inflammatory protein 1β (MIP-1β), but not MIP-1α, in MDMs by Nef expression was considerably suppressed by Lenti shNef366, which suggests that HIV-1 dissemination to T cells through its interaction with HIV-1–infected MDMs can also be controlled by Lenti shNef366. Thus, lentivirus-mediated shRNA expression targeting the U3-overlapping region of HIV *nef* represents a feasible approach to genetic vaccine therapy for HIV-1. (Blood. 2006;108:3305-3312)

Introduction

HIV Nef, which is uniquely conserved among HIV-1, HIV-2, and SIV, is essential for viral replication in vivo.[1] Nef is located at the 3′ end of the viral genome, partially overlapping the 3′ long terminal repeat (LTR). The *nef* gene is one of the earliest expressed genes during HIV-1 replication and is transcribed at particularly high levels, often accounting for up to 80% of HIV-1–specific RNA in the early stages of viral replication. The Nef protein is multifunctional, having been shown to be involved in the down-regulation of CD4 receptor molecules, cell apoptosis, and signal transduction.[2-6] From studies of HIV-infected individuals, accumulating evidence indicates that Nef plays an important, albeit currently not clearly understood, role in the pathogenesis of AIDS.[1,2,6,7]

Recent investigations have shown that Nef has evolved macrophage-specific functions, such as the recruitment of T cells to sites of infection.[8] Macrophages expressing Nef secrete a high level of macrophage inflammatory protein 1α (MIP-1α) and MIP-1β, thus recruiting peripheral T cells to lymph nodes. More recently it was shown that Nef regulates the release of paracrine factors from macrophages[9]; at least 2 proteins have been identified, which enhance lymphocyte susceptibly to HIV-1 infection in the absence of cell-cycle progression. These results provide ample evidence that Nef functions as a virulence factor that contributes to the manifestation of the clinical symptoms of immunodeficiency. Thus, any therapeutic intervention aimed at either completely blocking or at least partially reducing the expression of *nef* during HIV infection would likely enhance the ability of the immune system to fight HIV infection.

Sequence-specific degradation of viral mRNA by the process of RNAi is a mechanism for selectively inhibiting the synthesis of viral proteins that are critical for HIV-1 replication. RNAi therapy is based on an existing mechanism of gene regulation that is ubiquitous in plants and animals, in which targeted mRNAs are degraded in a sequence-specific manner.[10] Quite recently, several groups reported the use of RNAi to successfully inhibit HIV-1 replication.[11-15]

To study the effect of stable expression of short hairpin RNA (shRNA) against the U3-overlapping region of HIV-1 *nef* on virus replication and Nef-mediated cytokine regulation in primary macrophages, we established a lentivirus vector system expressing HIV-specific shRNAs. We show that HIV replication in primary macrophages was considerably suppressed following transfection of shRNAs targeting the U3-overlapping region of genomic HIV *nef*. Moreover, RNAi was able to control CC-chemokine

From the Department of Immunology, National Institute of Infectious Diseases, Toyama, Shinjuku-ku, Tokyo; Subteam for Manipulation of Cell Fate, BioResource Center, RIKEN Tsukuba Institute, Tsukuba; Department of Molecular Virology, Bio-Response, Tokyo Medical and Dental University, Bunkyo-ku, Tokyo; AIDS Research Center, National Institute of Infectious Diseases, Shinjuku, Tokyo; and Division of Cellular and Molecular Biology, Department of Cancer Biology, Institute of Medical Science, University of Tokyo, Shirokane-dai, Minato-ku, Tokyo, Japan.

Submitted April 6, 2006; accepted June 29, 2006. Prepublished online as *Blood* First Edition Paper, July 20, 2006; DOI 10.1182/blood-2006-04-014829.

Supported by a grant from the Ministry of Health, Labor, and Welfare of Japan and from the Japan Health Sciences Foundation.

The authors declare no competing financial interests.

T.Y. and Y.T.-Y. performed laboratory experiments, data management, and the biostatistical analysis; T.Y., Naoki Y., J.-i.I., and Y.T.-Y. were responsible for the general design of the study; H.M. and Norio Y. were responsible for the design of the specific parts on lentivirus vectors and quantitative PCR analysis, respectively; T.Y., Y.T.-Y., and J.-i.I. were involved in the interpretation of the results and general outline of the paper; and T.Y. and Y.T.-Y. wrote the article.

Reprints: Yasuko Tsunetsugu-Yokota, Department of Immunology, National Institute of Infectious Diseases, Toyama 1-23-1, Shinjuku-ku, Tokyo 162-8640, Japan; e-mail: yyokota@nih.go.jp.

The publication costs of this article were defrayed in part by page charge payment. Therefore, and solely to indicate this fact, this article is hereby marked "advertisement" in accordance with 18 USC section 1734.

production associated with Nef expression in HIV-1–infected macrophages. Thus, lentivirus-vector–based RNAi of the *U3*-overlapping region of HIV-1 *nef* might have potential usefulness as a genetic vaccine against HIV-1 infection.

Materials and methods

Construction of plasmids

To express gene-specific shRNAs under the human U6-RNA promoter, sense and antisense oligonucleotides 47 bp in length were ligated into pENTR/U6 (Invitrogen, Carlsbad, CA). The sequences of the oligonucleotides were as follows: *lacZ*, sense oligonucleotide, 5′-caccgctacacaaatcagcgatttcgaaaaatcgctgatttgtgtag-3′, and antisense oligonucleotide, 5′-aaaactacacaaatcagcgatttttcgaaatcgctgatttgtgtagc-3′; *Nef366* (nucleotides 366-385 of the HIV-1_{NL432} *nef* ORF overlapping the 3′ LTR), sense oligonucleotide, 5′-caccgattggcagaactacacaccaagagagtgtgtagttctgccaatc-3′, and antisense oligonucleotide, 5′-aaaagattggcagaactacacactctcttggtgtgtagttctgccaatc-3′. The resulting entry vectors were termed pENTR/shLacZ and pENTR/shNef366, respectively.

A Gateway-compatible (Invitrogen) HIV-1–based vector, pCS-RfA, containing elongation factor 1α promoter (EF-1α)–driven green fluorescent protein (EGFP) (pCS-RfA-EG),[16] was used to construct the lentivirus vectors, pCS-EG/shLacZ and pCS-EG/shNef366, according to the manufacturer's instructions (Invitrogen).

Cell culture and transfection

The human cell line 293T and human monocytic cell lines U937 and U1[17] were maintained in Dulbecco modified Eagle medium (DMEM) and RPMI 1640 medium (Gibco, Grand Island, NY), respectively, supplemented with 10% heat-inactivated fetal calf serum (FCS), penicillin (100 μg/mL), and streptomycin (100 μg/mL). To establish CCR5$^+$ CEMx174 cells expressing EGFP driven by HIV-LTR, CEMx174 cells were transfected with pEF-BOSbst-HuCCR5 and pHIV-1 LTR-EGFPpuro (kind gifts from M. Tatsumi, National Institute of Infectious Diseases, Tokyo, Japan) and CEMx174 CCR5/LTR-EGFP cells were established.

HeLa-CD4 cells (obtained from the National Institutes of Health AIDS Reagent Program) were transfected with pEF-Nef bst, and Nef-expressing HeLa-CD4 cells were established (HeLa-CD4-Nef).

RNAi target site selection

A Web-based program for designing siRNA targets (Promega, Madison, WI), BLOCK-iT RNAi Target Designer (Invitrogen), and the National Center for Biotechnology Information Web site were used for the selection of siRNA and shRNA sequences, and for BLAST searches. Stealth siRNAs were synthesized (Figure 1) and HeLa-CD4-Nef cells were transfected with 2.5 μL stealth siRNA complexed to 2.5 μL Lipofectamine 2000 (Invitrogen) according to the manufacturer's instructions. Total RNA was extracted and analyzed by quantitative reverse transcription–polymerase chain reaction (qRT-PCR) using specific LUX primers (Invitrogen) and the SuperScript III Platinum One-Step Quantitative RT-PCR system (Invitrogen). The sequences of the qRT-PCR primers were as follows: *nef* forward, labeled at its 3′ terminus with a reporter fluorophore 6-carboxyfluorescein (FAM), 5′-cagcagagtgtgattggatggcctgcFAMg-3′; *nef* reverse, 5′-tggctcagctcgtctcattctt-3′; *ef-1α* forward labeled at its 3′ terminus with a reporter fluorophore 6-carboxy-4′,5′-dichloro-2′,7′-dimethoxyfluorescein (JOE), 5′-gaaccacaagtgctaacatgccttggJOEtc-3′; *ef-1α* reverse, 5′-agcgtggttccactggcatt-3′. The reactions were performed using an Mx3000P (Stratagene, La Jolla, CA).

For Western blot analysis, cell lysates were prepared, subjected to 12.5% sodium dodecyl sulfate–polyacrylamide gel electrophoresis (SDS-PAGE), and immunoblotted with anti-Nef monoclonal antibody (mAb; F3, a kind gift from Dr Y. Fuji, Graduate School of Pharmaceutical Science, Nagoya City University, Nagoya, Japan). The blot was reacted with biotinylated goat anti-mouse IgG antibody (Jackson ImmunoResearch, West Grove, PA), then with streptavidin-POD (Roche, Indianapolis, IN).

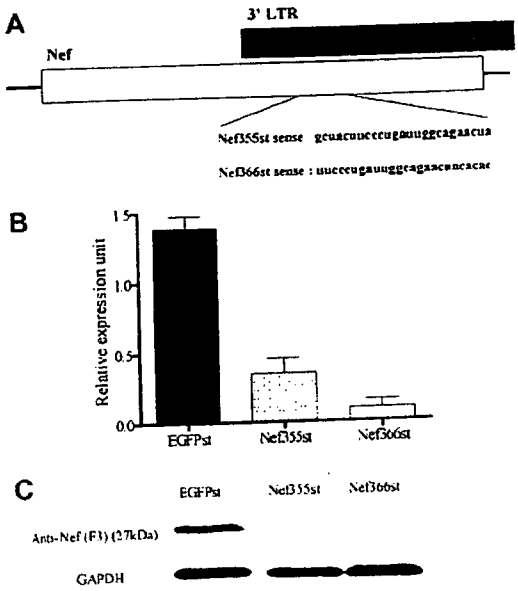

Figure 1. siRNA target sequences in *nef*. (A) Targets of siRNAs against the U3-overlapping region of HIV-1_{NL432} Nef and their sequences. Nef-expressing HeLa CD4 cells were transfected either with 2.5 μM *egfp* siRNAs (control: EGFPsi) or *nef* siRNAs (Nef355st or Nef366st). At 48 hours after transfection, these cells were lysed to obtain total RNA and protein. (B) Total RNA was extracted and analyzed by qRT-PCR. The level of *nef* mRNA expression was normalized with that of elongation factor 1α (EF-1α) mRNA expression (*nef*/EF-1α). The data represent the expression level of *nef* mRNA relative to that of the control as 100%. The data represent the average ± SD of 3 independent experiments. (C) The cell lysates were subjected to 12.5% SDS-PAGE and immunoblotted with anti-Nef mAb.

Proteins were visualized by the SuperSignal Western Dura Extended Duration Substrate (Pierce, Rockford, IL) using an LAS3000 analyzer (Fuji Film, Tokyo, Japan).

Preparation of lentivirus vector

The lentivirus shRNA expression vectors were produced by transient transfection of 293T cells with a self-inactivating (SIN) vector construct, VSV-G- and Rev-expressing plasmid pCMV-VSV-G-RSV-Rev, and the packaging construct pCAG-HIVgp using the calcium phosphate precipitation method.[16] The lentiviral vector was concentrated by ultracentrifugation and the final solution was assayed for p24 antigen by an in-house enzyme-linked immunosorbent assay (ELISA).[18] The infectivity was determined by using 293T cells based on the EGFP expression.

Preparation of HIV-1 virus stocks

To prepare HIV-1, COS-7 cells were transfected with either pNL432, pNF462 (a kind gift from A. Adachi, Tokushima University, Tokushima, Japan), or pNF462dNef, in which the *nef* gene was deleted by digestion with *Xho*I and *Kpn*I, as described previously.[18]

Primary MDM culture

From peripheral blood mononuclear cells (PBMCs) of healthy, HIV-1$^-$ donors, CD14$^+$ monocytes were enriched using a magnetic-activated cell sorter (MACS; Miltenyi Biotec, Cologne, Germany) as described.[18] Monocytes were cultivated in RPMI 1640 medium supplemented with 10% FCS, 5% human AB plasma, and 10 ng/mL macrophage colony-stimulating factor (M-CSF) for 1 week to allow differentiation into monocyte-derived macrophages (MDMs).

Kinetics of virus production in stable shRNA-expressing U937 cells

Stable shRNA-expressing cells were infected with HIV-1_{NL432} for 2 hours, then cells were washed 5 times. Culture supernatants were harvested at 3- or

4-day intervals and viral production was monitored by HIV of p24 Gag antigen ELISA kit (RETRO-TEC; ZeptoMetrix, Buffalo, NY).

Real-time RT-PCR (qRT-PCR) analysis of HIV-1 infection

HIV-1–infected cells were collected and total DNA was prepared 3, 8 and 12 hours after infection. For the detection and quantification of individual forms of HIV-1 DNA, oligonucleotide primer and probe sequences were designed specifically for the *Taq*Man assay as described elsewhere.[19] All probes (Biosearch Technologies, Novato, CA.) were 5′-labeled with the fluorophore FAM as the reporter dye, and 3′-labeled with Black Hole Quencher-1 (BHQ-1) as the quencher dye. The qRT-PCR analysis was performed on an Mx3000P (Stratagene) and the amount of HIV-1–specific DNA per cell was normalized to β-globin gene.

Kinetics of virus production in MDMs and reporter analysis

MDMs (2×10^5/well) were cultured in 48-well tissue-culture plates and infected either with wild-type HIV-1_{NF462} or HIV-$1_{NF462\Delta Nef}$. MDMs were infected with lentivirus at a multiplicity of infection (MOI) of 2 or 10 and washed extensively. The next day, cells were exposed to HIV-1 (5 ng/well) for 2 hours. Cell supernatants were harvested at 3- or 4-day intervals, and viral production was monitored by p24 antigen ELISA.

The cell-culture supernatants at 10 days after HIV infection were examined for infectivity, and 10 days after HIV infection, cell supernatants were collected (termed HIV-1/Lenti cont and HIV-1/Lenti shNef366). CEMx174 CCR5/LTR-EGFP cells were infected with HIV-1/Lenti cont or HIV-1/Lenti shNef366, and the number of HIV-1–infected EGFP$^+$ T cells was determined by fluorescence-activated cell sorter (FACS).

Detection of chemokines

For the detection of chemokine production in MDMs, the cytometric bead array (CBA) kit (BD Bioscience, San Jose, CA) was used, which measured 4 chemokines (IL-8, MIP-1α, MIP-1β, MCP-1) simultaneously.

Restimulation assay of lentivirus-transduced U1 cells

Latent HIV-1–infected U1 cells were transduced with Lenti cont or Lenti shNef366 at an MOI of 1. Two weeks later, EGFP$^+$ cells were sorted and stimulated with 1 ng/mL recombinant granulocyte-macrophage colony-stimulating factor (GM-CSF). Culture supernatants were collected at days 2 and 5, and the level of p24 antigen was measured by ELISA.

Results

siRNA suppresses *nef* mRNA and Nef protein expression

In the HIV-1 genome, *nef* is located at the 3′ end of the viral genome, partially overlapping the 3′ LTR (Figure 1A). Jacque and colleagues demonstrated previously that siRNA targeting of the 5′ region of *nef* (nucleotides 164-185) suppressed HIV replication.[20] Therefore, we selected 3 distinct regions of the HIV-1_{NL432} *nef* sequence using a Web-based program for designing DNA-directed RNAi systems, focusing on the Nef coding region overlapping the 3′ LTR. These were designated as Nef338, 366, and 479 based on the position of the first nucleotide of the siRNA. From initial screening experiments, we found that Nef366 was the most effective target site (data not shown).

The type 1 interferon response is an innate defense mechanism in eukaryote cells against viral infection. It has been shown that some types of siRNA induce type 1 interferon, which in turn mediates the gene-specific effect of RNAi.[21-23] The stealth siRNA system was developed to avoid the interferon response to siRNA in cells (Invitrogen manual). We prepared synthetic stealth siRNAs, designated Nef355st and Nef366st, and a control siRNA designated EGFPst, to determine the effect of RNAi using sequences based on Nef366 (the U3-overlapping region of the Nef-coding region). Neff355st was synthesized based on a Web-based computer program for generating stealth siRNA (Invitrogen), whereas Nef366st represents a slightly modified version of the stealth target site (6-nucleotide difference), so that it conformed to the target sequence as described. These stealth Nef siRNA sequences differed by only 5 nucleotides (Figure 1A).

We established a stable Nef-expressing HeLa-CD4 clonal cell line, designated as HeLa-CD4-Nef. HeLa-CD4-Nef cells were transfected either with 2.5 μM EGFPst or *nef* stealth siRNAs (Nef355st or Nef366st), and harvested 48 hours after transfection. Total RNA was extracted and the level of *nef* mRNA was measured by qRT-PCR. We observed that transfection with Nef366st reduced *nef* mRNA expression more than 90% (Figure 1B), whereas Nef355st suppressed the level of *nef* mRNA approximately 80%, compared with EGFPst controls. When cell lysates of the transfected cells were analyzed by Western blot, we found that both Nef366st and Nef355st suppressed Nef protein levels to below the detection limit of the assay (Figure 1C). Taken together, these results clearly showed that Nef366 is an efficient target sequence for the inhibition of *nef* gene expression by siRNA.

shRNA suppresses *nef* mRNA and Nef protein expression

To assess the effect of endogenous expression of Nef366 siRNA, we constructed expression vectors that encoded shRNAs corresponding to Nef366, or *lacZ* as a control, driven by the human U6 polymerase III promoter, designated as pENTR/shNef366 and pENTR/shLacZ, respectively (Figure 2A). HeLa-CD4-Nef cells were transfected with either pENTR/shNef366 or pENTR/shLacZ by FuGene6 reagent (Roche) and cells were harvested 72 hours after transfection. Total RNA was extracted and analyzed by qRT-PCR. We observed that the level of *nef* mRNA was suppressed by approximately 80% in cells transfected with pENTR/shNef366 (Figure 2B). Western blot analysis confirmed that pENTR/shNef366 strongly suppressed Nef protein levels as well (data not shown). These results indicated that promoter-driven endogenous

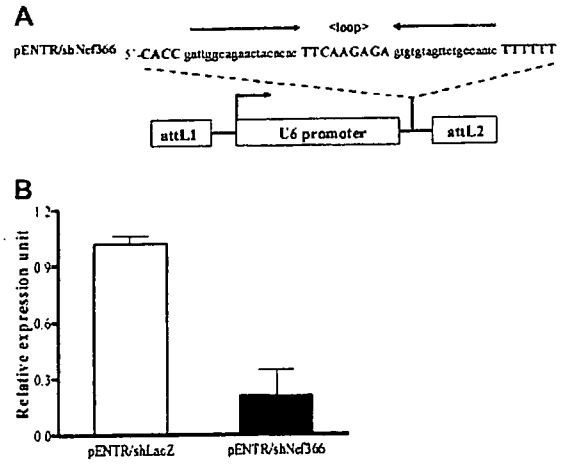

Figure 2. RNAi by transfection with shRNA expression vectors. (A) Schematic of the expression vectors (pENTR/shRNA) encoding shRNAs of Nef366 or *lacZ*, designated as pENTR/shNef366 and pENTR/shLacZ, respectively, in which expression is driven by the human U6 polymerase III promoter. (B) Nef-expressing HeLa-CD4 cells were transfected either with 1.0 μg pENTR/shNef366 or pENTR/shLacZ and cells were harvested 72 hours after transfection. Total RNA was extracted and analyzed by qRT-PCR. The data represent the average ± SD of 3 independent experiments.

expression of shNef366 was able to mediate RNAi of *nef* in HeLa-CD4-Nef cells.

Inhibition of HIV-1 replication in U937 cells by lentivirus-based shRNA expression

The transfection efficiency of the entry vectors used in suspension cells was quite low, and the objective here is to introduce siRNAs into primary macrophages. Therefore we constructed HIV-1–based lentivirus vectors expressing Nef366 shRNA or shRNA targeting lacZ as a control (Lenti shNef366 and Lenti control) using Gateway technology. The structure of the lentivirus vector used in the following studies is illustrated in Figure 3A.

To test whether Nef366 shRNA was able to efficiently block HIV-1 replication, we infected U937 cells with Lenti shNef366 or Lenti control, both of which encoded GFP driven by the EF-1α promoter (EGFP), at an MOI of 1. Two weeks after infection, nearly 30% of the cells stably expressed EGFP (Figure 3B upper panel). We sorted the EGFP$^+$ cells by fluorescence-activated cell sorter (FACSaria; BD Biosciences), after which the purity of the Lenti control– and Lenti shNef366–transfected, EGFP$^+$ cells was 97.2% and 99.7%, respectively (Figure 3B lower panel; U937/Lenti cont and U937/Lenti shNef366). The purified cell populations were then infected with 2 inoculation doses of HIV-1 (Figure 3C upper and lower panels; p24: 20 ng and 100 ng, respectively). The culture supernatants were collected at 3- or 4-day intervals, and the level of p24 antigen was measured by ELISA. We observed that at both inoculation doses HIV-1 replication in U937 cells was inhibited by Lenti shNef366, especially at the peak of HIV-1 production. The reverse transcriptase activity was also measured in parallel, and the result was consistent with that of p24 ELISA (data not shown). The inhibition of HIV-1 replication was sustained at least for 1 week, following which HIV-1 production gradually decreased in all cell populations, presumably because of the cytopathic effect of HIV-1 infection.

To further evaluate the effect of RNAi on the early steps of HIV-1 infection, we prepared cell lysates at different time points after inoculation (3, 8, and 12 hours after infection) and analyzed the level of reverse transcription activity by measuring the amount of different forms of proviral DNA (HIV-1 *2LTR* and *U5-Gag*) by the qRT-PCR. The copy number of these proviral DNA forms decreased in U937/Lenti shNef366 cells, relative to that seen in U937/Lenti control cells at all time points. The amount of these DNA forms normalized to β-globin gene at 12 hours after HIV-1 infection is depicted in Figure 3D. The copy number of *2LTR* and *U5-Gag* was 16.9% and 13.4% of control, respectively. These results suggested that the inhibition of HIV-1 replication occurred early after virus entry, presumably during uncoating or reverse transcription, not integration.

A type I interferon response has been shown to be induced by synthetic siRNAs via protein kinase R- (PKR) or toll-like receptor 7 (TLR 7)–mediated signaling pathways.[21-23] To eliminate the possibility that we were generating an interferon response following shRNA expression in our system, we analyzed the level of 2′ 5′-oligoadenylate synthetase mRNA expression in Lenti shNef366–infected U937 cells by qRT-PCR. We detected no such message (data not shown), indicating that the interferon response plays a

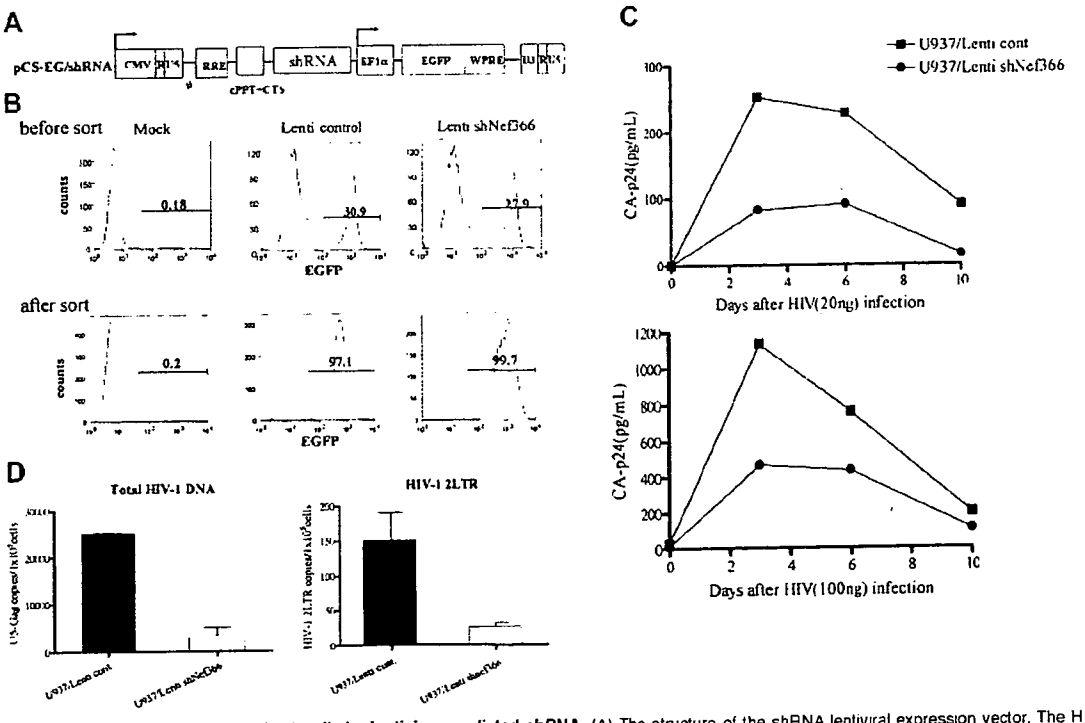

Figure 3. Inhibition of HIV-1 replication in U937 cells by lentivirus-mediated shRNA. (A) The structure of the shRNA lentiviral expression vector. The HIV-1–based lentivirus vector for expressing shRNA was constructed using Gateway technology. pCS-EG/shRNA consisted of U6-shRNA upstream of an EF1α promoter–driven EGFP expression cassette, which allowed simultaneous expression of shRNA and EGFP. (B) U937 cells were infected with lentivirus expressing either shNef366 (Lenti shNef366) or shLacZ (Lenti control) at an MOI of 1. After 2 hours of infection, cells were washed and maintained in culture. Cells expressing EGFP were analyzed by FACS, and EGFP$^+$ cells were collected. EGFP$^+$ cells were analyzed by FACSaria 1 week later (designated as U937/Lenti control and U937/Lenti shNef366). (C) U937/Lenti cont or U937/Lenti shNef366 cells (1×10^5/well) were infected with HIV-1_{NL432}, and the culture supernatants of these cells were collected at 3- or 4-day intervals after infection. The level of p24 antigen in the culture supernatants was measured by ELISA. (D) HIV-1–infected cells were collected and total DNA was prepared 12 hours after infection. Total HIV-1 and 2LTR DNA was analyzed by qRT-PCR. The amount of HIV-1–specific DNA per cell was normalized to β-globin gene expression. The data represent the average ± SD of 3 independent experiments.

minimal role, if any, in the observed inhibitory effect on HIV replication by Lenti shNef366.

Lentivirus-based nef shRNA inhibits HIV-1 replication and affects chemokine production in MDMs

Swingler and coworkers reported that HIV-1 Nef expression in macrophages mediated lymphocyte chemotaxis and activation through the induction of MIP-1α and MIP-1β expresion.[8] To determine the effect of Nef expression during HIV-1 infection in MDMs, we infected MDMs with wild-type HIV-1_{NF462} or the corresponding *nef* gene-deletion mutant, HIV-1_{NF462}dNef, and assessed the kinetics of virus replication by p24-specific ELISA. Representative results from 2 donors are shown in Figure 4A. We consistently observed that the level of HIV-1_{NF462} replication was 2- to 6-fold higher than that of HIV-1_{NF462}dNef in MDMs. These results were consistent with those reported by Swingler et al.[9] Although no apparent T-cell damage was observed during cultivation for 3 weeks following HIV-1 infection, the amount of virus production gradually decreased. We analyzed chemokine production in MDMs infected with HIV-1 wild-type and *nef*-deleted HIV-1 at days 10, 14, and 17 after infection. The level of chemokine production in uninfected MDMs varied depending on the donor, but both donors produced a high level of IL-8 and monocyte chemotactic protein-1 (MCP-1), and a low level of MIP-1α and MIP-1β (data not shown). HIV infection per se, independent of the presence or absence of Nef, did not affect this trend, in that the levels of these chemokines, with the exception of MIP-1β, were only slightly affected by HIV infection. Notably, virus replication resulted in an increased production of MIP-1β, which peaked at 14 days after infection, in parallel with the peak of viral replication. Figure 4B shows the results of the analysis of the levels of MIP-1β and MIP-1α in the 2 donors. HIV-1 infection induced a 2-fold increase in the level of MIP-1β compared with mock-infected MDMs. In contrast, infection with Nef-deleted HIV-1 caused a reduction in the level of MIP-1β in the MDMs from both donors, indicating that Nef is responsible for the up-regulation of MIP-1β, but does not affect MIP-1α, MCP-1, or IL-8 production.

To examine whether shRNAs against the U3-overlapping region of *nef* were able to block HIV-1 replication in MDMs, we infected MDMs with Lenti control or Lenti shNef366, at an MOI of 10 or 2 (Figure 5A left and right panels, respectively). After 2 hours of incubation, cells were extensively washed and cultivated overnight, and the following day, they were infected with HIV-1_{NF462}. Culture supernatants were collected every 3 or 4 days and the level of p24 antigen was measured by ELISA. Of note, despite the extensive washing after lentivirus infection, the level of p24 was quite high up to 7 days after HIV-1 infection. We detected a second peak of virus production, which we interpreted as true HIV-1 replication in MDMs transduced with lentiviral vectors expressing shRNAs. In addition, presumably because of the toxic effect of infection by lentivirus pseudotyped with VSV, the level of p24 antigen was lower than that in MDMs infected with HIV-1 virus. Nevertheless, we observed a similar level of inhibition of HIV-1 replication in MDMs by Lenti shNef366 at 2 different doses of infection (Figure 5A), and the inhibition was maintained for at least 3 weeks after HIV-1 infection.

Macrophages can mediate efficient infection of lymphocytes *in trans*,[9,24] suggesting that macrophages serve as a major reservoir and vehicle for HIV-1 dissemination. We were interested in whether the progeny virus produced from MDMs harboring Nef366 shRNA maintained their ability to infect T cells. Supernatants from MDM cells transduced with Lenti control or Lenti shNef366 were collected 10 days after HIV infection, and the level of p24 antigen was measured and used to quantitate the amount of HIV present. These sources of HIV were designated as HIV/Lenti cont or HIV/Lenti shNef366. Using CEMx174 CCR5/LTR-EGFP cells as indicator cells, we estimated the infectivity of HIV/Lenti cont or HIV/Lenti shNef366 by analyzing the number of $EGFP^+$ T cells following infection (Figure 5B). Compared with HIV-1/Lenti cont, HIV-1/Lenti shNef366 had a significant loss of infectivity in $CCR5^+$ T cells. Our results suggested that Lenti shNef366 has the potential to protect HIV-1 dissemination to T cells by HIV-1–infected MDMs

We also examined the level of chemokine production following HIV infection of MDMs transduced with shRNA lentivirus vectors. Although the basal level of MIP-1α and MIP-1β production was slightly increased following lentivirus infection, the level of MIP-1β decreased in Lenti shNef366 cells compared with Lenti control (Figure 5C). The levels of MCP-1 and IL-8 were either unaffected or somewhat restored by Lenti shNef366 (data not shown).

Lentivirus-based nef shRNA protects progression from latent HIV-1 infection to productive infection

Latent HIV-1 infection can be established following provirus integration into the host genome.[25-27] A small number of infected cells re-enter the resting stage, harboring an integrated copy of the HIV-1 genome. These latent HIV-infected cells represent a barrier to successful virus eradication because subsequent cytokine or

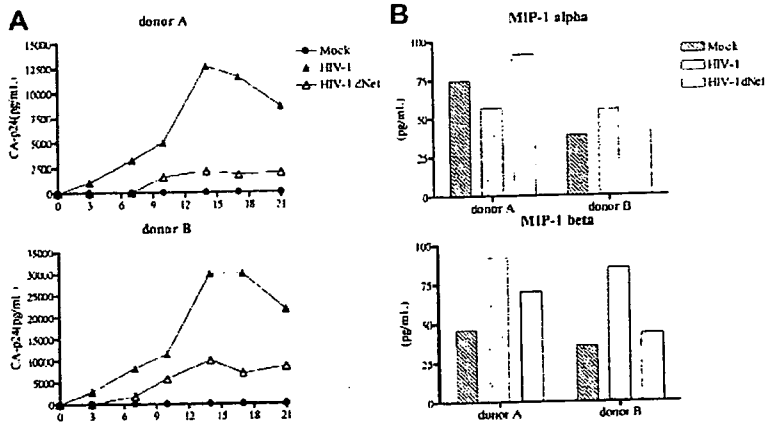

Figure 4. The effect of Nef expression during HIV-1 infection in MDMs. (A) MDMs (2×10^5/well) of 2 donors were infected either with wild-type HIV-1_{NF462} or HIV-$1_{NF462dNef}$. The supernatants of these wells were harvested at 3- or 4-day intervals after infection, and viral production was monitored by sequential quantitation of p24 by ELISA. (B) The CBA kit was used to measure the level of chemokines (MIP-1α and MIP-1β) in cell supernatants 14 days after HIV infection.

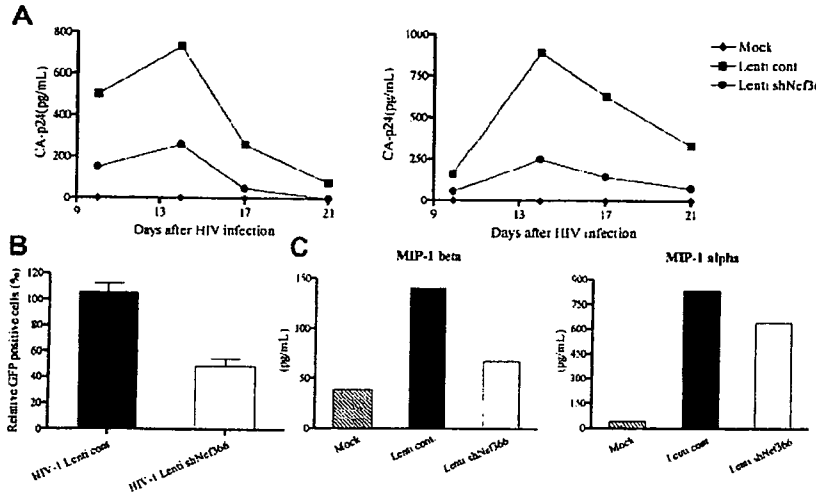

Figure 5. Lentivirus-expressed nef shRNA inhibits HIV-1 replication and affects chemokine production in MDMs. (A) MDMs were transduced with Lenti cont or Lenti shNef366 at an MOI of 2. At 2 hours after infection, cells were washed twice, then cultured for another 24 hours, at which point the cells were infected with HIV-$1_{NL\,4\text{-}3}$. The culture supernatants were collected at 3- or 4-day intervals after HIV infection, and the level of p24 antigen was measured by ELISA. (B) MDMs transduced either with Lenti control or Lenti shNef366 were infected with HIV-1 and supernatants were collected 10 days after infection and designated as HIV-1 Lenti cont and HIV-1 Lenti shNef366, respectively. CEMx174 CCR5/LTR-EGFP cells were infected either with HIV-1 Lenti cont or HIV-1 Lenti shNef366 and GFP$^+$, HIV-1–infected T cells were analyzed by FACS 48 hours later. The data represent the average ± SD of 3 independent experiments. (C) The culture supernatants of MDMs transduced with lentivirus vectors were collected 14 days after infection and the levels of the chemokines MIP-1α and MIP-1β were measured.

other stimuli can reactivate viral gene expression, and reinitiate HIV-1 replication.[28-31] We were interested in whether Lenti shNef366 was able to regulate the progression of latent HIV-1 infection to productive infection in U1 cells.[17] U1 cells are U937 cells in which a latent HIV-infection has been established, and HIV-1 replication can be induced in these cells on appropriate activation. We transduced U1 cells with Lenti control or Lenti shNef366 at an MOI of 1. After 2 hours of infection, cells were extensively washed and maintained in culture. Two weeks after transduction, the cells were sorted by FACSaria, and the EGFP$^+$ cell population was stimulated with 1 ng/mL recombinant GM-CSF. Culture supernatants were collected at different time points (days 2 and 5) and the level of p24 antigen was measured by ELISA. As shown in Figure 6, the levels of p24 antigen were dramatically decreased in U1 cells harboring Lenti shNef366 at all time points examined.

Discussion

In this study, we constructed an shRNA expression system that targeted HIV *nef* gene sequences that overlap the 3′ LTR U3 (Nef366) and showed that Nef366 shRNA had a strong inhibitory effect on *nef* gene expression in Nef-expressing HeLa-CD4 cells. Furthermore, expression of shNef366 in monocytic cell lines strongly inhibited the replication of HIV-1 at an early stage of HIV infection. The rational for using shNef366 to target HIV *nef* was several-fold. Because the U3 region is required during reverse transcription for first template transfer and integration of the viral genome into the host genome, siRNA targeting of the U3 region may induce not only specific degradation of *nef* mRNA, but also inhibit HIV-1 reverse transcription. Furthermore, although others have observed escape mutations in RNAi experiments targeting *nef* or *tat*,[32,33] the nef/U3 sequence we targeted is highly conserved as discussed in the paragraph after the next one. If a mutation were to occur in the U3 region, it would affect the overall transcription efficiency of HIV-1 after integration because the U3 region of the HIV-1 LTR contains the transcription initiation or promoter/enhancer sites that are essential for efficient HIV transcription. Of note, the strategy used Jacque et al[20] using siRNA targeting of the 5′ region of *nef* turned out to induce an escape mutant.[33] Although we did not extensively test for the emergence of escape mutants, targeting the 3′ LTR U3-overlapping region of *nef* (Nef366) represented a potentially potent strategy for controlling HIV-1 replication.

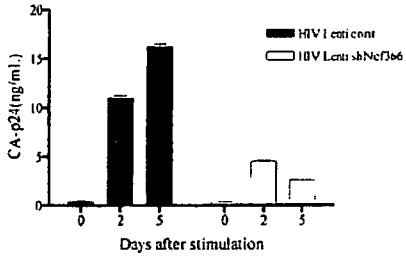

Figure 6. The effect of Lenti shNef366 on latent HIV-1 infection. Latent HIV-1–infected U1 cells were transduced with Lenti control or Lenti shNef366 at an MOI of 1. Two weeks after infection, EGFP$^+$ cells were sorted by FACSaria, and EGFP$^+$ cells were stimulated with 1 ng/mL recombinant GM-CSF. Cell-culture supernatants were collected 0, 2, and 5 days after stimulation, and the level of p24 antigen was measured by ELISA. The data represent the averages ± SDs of 3 independent experiments.

Macrophages are one of the major target cell populations in the early phase of HIV-1 infection, when R5 viruses predominate.[34] HIV-1 replication in macrophages is usually slow and less cytopathic compared with that in activated T cells, allowing the virus to survive long after infection. Thus, macrophages serve as one of the reservoirs for HIV in an infected individual.[35] Therefore, therapeutic strategies that target macrophages are promising approaches to the control of persistent HIV-1 infection in vivo. Taking advantage of the lentivirus expression system, which is an efficient way to introduce a desired gene into primary cells, we were able to show that expression of Nef366 shRNAs in primary MDMs inhibited HIV-1 replication in these cells.

In this context, several groups have demonstrated that RNAi, mediated by the introduction of HIV-specific siRNA duplexes, can inhibit viral replication in T cells, although the effect was transient.[20,36-38] Das et al were able to show a stable inhibitory effect on viral replication using a murine retrovirus vector expressing Nef-specific siRNAs in T-cell lines. However, the block in virus replication was not absolute and escape mutants emerged.[33] These previous results prompted us to develop a novel strategy of RNAi-mediated inhibition of HIV infection that did not induce a type I interferon and had a stable, long-term effect. We chose to

transduce Nef366 shRNA into low or nondividing primary macrophages, as opposed to actively proliferating T cells, using a lentivirus expression vector, and were able to demonstrate RNAi effect during macrophage cultivation for 3 weeks. Using an alignment of 200 HIV-1 sequences obtained by BLAST search analysis, only one base mismatch in the Nef366 region was detected in a subtype A virus (GenBank no. AB098332 and no. AB098333, HIV-1 UG029). Further study will be required to determine whether this subtype A virus is resistant to shRNA Nef366. Because Nef/LTR is in a completely conserved region, at least among subtype B viruses, this region might have quite an important function for HIV-1 replication. We speculate that if escape mutants were to emerge in the presence of lentiviral-shRNA Nef366, the compensatory mutation would occur outside of this region.

Importantly, using this system, we were also able to demonstrate a decrease in the infectivity of HIV-1 produced from infected MDMs. This attenuation effect is potentially significant because it implies that lentivirus-mediated RNAi may also reduce transmissibility of HIV-1 overall. However, in light of the significant problem of viral escape during chronic HIV infection, it may become necessary to combine multiple sites of siRNAs targeting the *nef-U3* region in the future.

Control of the latent phase of HIV infection is a key issue for effective therapeutic intervention. We demonstrated here that Lenti shNef366 was able to suppress the reactivation of HIV from latently infected cells. The expression of integrated HIV-1 in latently infected cells is controlled at the level of transcription by cellular factors and the viral transactivator Tat, both of which act through the HIV-1 LTR.[39] Transcription of integrated viral RNA is initiated at the R region of the 5′ LTR. The fact that shNef366, which targeted the U3-overlapping region of Nef, was effective in latently infected cells, suggests that shNef366 can directly target cleavage of *nef* mRNAs or total viral RNAs at the 3′ end. Therefore, our lentivirus-based shRNA expression system appears to be able to control both early and latent HIV-1 infection.

MIP-1α and MIP-1β are ligands of the HIV-1 coreceptor, CCR5. Through interaction with the CCR5 receptor, they promote the maturation of Th1 cells.[40,41] Swingler et al reported that MIP-1α and MIP-1β were induced by Nef in macrophages during HIV infection and that culture supernatants derived from Nef-expressing macrophages induced both chemotaxis and activation of resting T lymphocytes, enabling productive HIV-1 infection of those T cells.[8] These and other results have led to a model of HIV infection in which expression of Nef in HIV-infected MDMs enhances the secretion of MIP-1β, which recruits mainly $CCR5^+$ Th1 cells, resulting in the expansion of R5 tropic HIV-1 during macrophage–T-cell interactions. Our results were partially consistent with this model because the degradation of *nef* mRNA expression resulted in the decreased MIP-1β production. Of note, the production of MIP-1α in our system appeared to be unaffected by Nef expression but was induced by lentivirus infection. Because the production of MIP-1α in HIV-infected MDMs was similar to that in uninfected MDMs, it seems likely that MIP-1α production was enhanced by a non–HIV-specific component of the lentivirus expression system, perhaps VSV-G protein. Although the levels of MCP-1 and IL-8 varied depending on the donor and were independent of Nef expression, we cannot rule out the possibility that other unknown chemokines are induced by Nef. Any such dysregulated chemokine production by Nef expression in macrophages might provide an appropriate environment for HIV to establish an efficient infection and dissemination.

In summary, we demonstrated the feasibility of using lentiviral expression vectors to express shRNAs against the U3-overlapping region of *nef* in primary MDMs, as a type of intracellular immunization and potential gene therapy approach against HIV-1. Future development of an AIDS vaccine based on the specific inhibition of viral gene expression combined with existing therapeutic strategies may provide keys to help eradicate HIV.

Acknowledgments

We thank Masayuki Ishige and Rieko Iwaki for their excellent technical assistance.

References

1. Kestler HW 3rd, Ringler DJ, Mori K, et al. Importance of the nef gene for maintenance of high virus loads and for development of AIDS. Cell. 1991;65:651-662.
2. Agopian K, Wei BL, Garcia JV, Gabuzda D. A hydrophobic binding surface on the human immunodeficiency virus type 1 Nef core is critical for association with p21-activated kinase 2. J Virol. 2006;80:3050-3061
3. Fackler OT, Baur AS. Live and let die: Nef functions beyond HIV replication. Immunity. 2002;16:493-497.
4. Geyer M, Fackler OT, Peterlin BM. Structure–function relationships in HIV-1 Nef. EMBO Rep. 2001;2:580-585
5. Steffens CM, Hope TJ. Recent advances in the understanding of HIV accessory protein function. AIDS. 2001;15(suppl 5):S21-S26.
6. Na YS, Yoon K, Nam JG, et al. Nef from a primary isolate of human immunodeficiency virus type 1 lacking the EE(155) region shows decreased ability to down-regulate CD4. J Gen Virol. 2004;85:1451-1461.
7. Deacon NJ, Tsykin A, Solomon A, et al. Genomic structure of an attenuated quasi species of HIV-1 from a blood transfusion donor and recipients. Science. 1995;270:988-991
8. Swingler S, Mann A, Jacque J, et al. HIV-1 Nef mediates lymphocyte chemotaxis and activation by infected macrophages. Nat Med. 1999;5:997-103.
9. Swingler S, Brichacek B, Jacque JM, Ulich C, Zhou J, Stevenson M. HIV-1 Nef intersects the macrophage CD40L signalling pathway to promote resting-cell infection. Nature. 2003;424:213-219.
10. Hannon GJ. RNA interference. Nature. 2002;418:244-251.
11. Coburn GA, Cullen BR. Potent and specific inhibition of human immunodeficiency virus type 1 replication by RNA interference. J Virol. 2002;76:9225-9231.
12. Lee MT, Coburn GA, McClure MO, Cullen BR. Inhibition of human immunodeficiency virus type 1 replication in primary macrophages by using Tat- or CCR5-specific small interfering RNAs expressed from a lentivirus vector. J Virol. 2003;77:11964-11972.
13. Novina CD, Murray MF, Dykxhoorn DM, et al. siRNA-directed inhibition of HIV-1 infection. Nat Med. 2002;8:681-686
14. Qin XF, An DS, Chen IS, Baltimore D. Inhibiting HIV-1 infection in human T cells by lentiviral-mediated delivery of small interfering RNA against CCR5. Proc Natl Acad Sci U S A. 2003;100:183-188.
15. Song E, Lee SK, Dykxhoorn DM, et al. Sustained small interfering RNA-mediated human immunodeficiency virus type 1 inhibition in primary macrophages. J Virol. 2003;77:7174-7181.
16. Miyoshi H, Blomer U, Takahashi M, Gage FH, Verma IM. Development of a self-inactivating lentivirus vector. J Virol. 1998;72:8150-8157.
17. Folks TM, Justement J, Kinter A, Dinarello CA, Fauci AS. Cytokine-induced expression of HIV-1 in a chronically infected promonocyte cell line. Science. 1987;238:800-802.
18. Tsunetsugu-Yokota Y, Kato T, Yasuda S, et al. Transcriptional regulation of HIV-1 LTR during antigen-dependent activation of primary T cells by dendritic cells. J Leukoc Biol. 2000;67:432-440.
19. Yamamoto N, Tanaka C, Wu Y, et al. Analysis of human immunodeficiency virus type 1 integration by using a specific, sensitive and quantitative assay based on real-time polymerase chain reaction. Virus Genes. 2006;32:105-113.
20. Jacque JM, Triques K, Stevenson M. Modulation of HIV-1 replication by RNA interference. Nature. 2002;418:435-438.
21. Hornung V, Guenthner-Biller M, Bourquin C, et al. Sequence-specific potent induction of IFN-alpha by short interfering RNA in plasmacytoid dendritic cells through TLR7. Nat Med. 2005;11:263-270.
22. Bridge AJ, Pebernard S, Ducraux A, Nicoulaz AL,

Iggo R. Induction of an interferon response by RNAi vectors in mammalian cells. Nat Genet. 2003;34:263-264.

23. Sledz CA, Holko M, de Veer MJ, Silverman RH, Williams BR. Activation of the interferon system by short-interfering RNAs. Nat Cell Biol. 2003;5: 834-839.
24. Carr JM, Hocking H, Li P, Burrell CJ. Rapid and efficient cell-to-cell transmission of human immunodeficiency virus infection from monocyte-derived macrophages to peripheral blood lymphocytes. Virology. 1999;265:319-329.
25. Garcia-Blanco MA, Cullen BR. Molecular basis of latency in pathogenic human viruses. Science. 1991;254:815-820.
26. McCune JM. Viral latency in HIV disease. Cell. 1995;82:183-188.
27. Finzi D, Siliciano RF. Viral dynamics in HIV-1 infection. Cell. 1998;93:665-671.
28. Chun TW, Stuyver L, Mizell SB, et al. Presence of an inducible HIV-1 latent reservoir during highly active antiretroviral therapy. Proc Natl Acad Sci U S A. 1997;94:13193-13197.
29. Finzi D, Hermankova M, Pierson T, et al. Identification of a reservoir for HIV-1 in patients on highly active antiretroviral therapy. Science. 1997; 278:1295-1300.
30. Wong JK, Hezareh M, Gunthard HF, et al. Recovery of replication-competent HIV despite prolonged suppression of plasma viremia. Science. 1997;278:1291-1295.
31. Chun TW, Engel D, Mizell SB, Ehler LA, Fauci AS. Induction of HIV-1 replication in latently infected CD4+ T cells using a combination of cytokines. J Exp Med. 1998;188:83-91.
32. Boden D, Pusch O, Lee F, Tucker L, Ramratnam B. Human immunodeficiency virus type 1 escape from RNA interference. J Virol. 2003;77:11531-11535.
33. Das AT, Brummelkamp TR, Westerhout EM, et al. Human immunodeficiency virus type 1 escapes from RNA interference-mediated inhibition. J Virol. 2004;78:2601-2605.
34. Moore JP, Kitchen SG, Pugach P, Zack JA. The CCR5 and CXCR4 coreceptors—central to understanding the transmission and pathogenesis of human immunodeficiency virus type 1 infection. AIDS Res Hum Retroviruses. 2004;20:111-126.
35. Aquaro S, Calio R, Balzarini J, Bellocchi MC, Garaci E, Perno CF. Macrophages and HIV infection: therapeutical approaches toward this strategic virus reservoir. Antiviral Res. 2002;55:209-225.
36. Capodici J, Kariko K, Weissman D. Inhibition of HIV-1 infection by small interfering RNA-mediated RNA interference. J Immunol. 2002; 169:5196-5201.
37. Dave RS, Pomerantz RJ. Antiviral effects of human immunodeficiency virus type 1-specific small interfering RNAs against targets conserved in select neurotropic viral strains. J Virol. 2004;78: 13687-13696.
38. Stevenson M. Dissecting HIV-1 through RNA interference. Nat Rev Immunol. 2003;3:851-858.
39. Cullen BR. HIV-1 auxiliary proteins: making connections in a dying cell. Cell. 1998;93:685-692.
40. Loetscher P, Uguccioni M, Bordoli L, et al. CCR5 is characteristic of Th1 lymphocytes. Nature. 1998;391:344-345.
41. Luther SA, Cyster JG. Chemokines as regulators of T cell differentiation. Nat Immunol. 2001;2:102-107.

Available online at www.sciencedirect.com
SCIENCE DIRECT
ELSEVIER
Biomedicine & Pharmacotherapy 60 (2006) 211–219
BIOMEDICINE & PHARMACOTHERAPY
http://france.elsevier.com/direct/BIOPHA/

Original article

Anti-RNA virus activity of polyoxometalates

Shiro Shigeta [a,b,*], Shuichi Mori [b], Toshihiro Yamase [c], Norio Yamamoto [d], Naoki Yamamoto [d]

[a] *Bureau of Prefectural Hospitals, Fukushima Prefecture*
[b] *Department of Microbiology, Fukushima Medical University School of Medicine*
[c] *Chemical Resources Laboratory, Tokyo Institute for Technology*
[d] *Department of Molecular Virology, Bio Response, Graduate School Tokyo Medical and Dental School*

Received 8 February 2006; accepted 7 March 2006
Available online 24 May 2006

Abstract

The anti-RNA virus activity of polyoxometalates (POM) is reviewed, with a special emphasis on the anti-respiratory virus activities. There are many causative agents of acute viral respiratory infections; and it is rather difficult to identify the relevant agent in a given case by rapid clinical means. During acute progress of infection before the definitive diagnosis is obtained physicians need to prescribe certain broad spectrum anti viral drugs. A titanium containing polyoxotungstate, PM-523 exhibited potent anti-influenza virus (FluV) A and anti-respiratory syncytial virus (RSV) activities in vitro. Therapeutic effect of FluV A infected mice with aerosol inhalation of PM-523 was proven. A vanadium substituted polyoxotungstate, PM-1001 has antiviral activity against FluV A, RSV, parainfluenza virus (PfluV) type 2, Dengue fiver virus, HIV-1 and SARS coronavirus in vitro. Thus, POMs have been proven to be broad spectrum and non-toxic anti-RNA virus agents in both in vitro and in vivo experiments and are promising candidates for first-line therapeutics in acute respiratory diseases.

Keywords: Polyoxometalates; Anti-RNA virus activity; Acute respiratory diseases

1. Introduction

The polyoxometalates (POM) are negatively charged clusters of inorganic substances principally comprised of oxide anions and early transition-metal cations. They have been shown to exhibit antiviral activity against several RNA viruses including the orthomyxoviruses, paramyxoviruses, flaviviruses, coronaviruses and retroviruses in vitro and in vivo. Some species of orthomyxoviruses, paramyxoviruses and coronaviruses are causative agents of respiratory infections and have been an active target for the broad spectrum antiviral agents. We examined several types of POM for anti-RNA virus activities and found some indeed have broad antiviral activities against the RNA viruses which cause acute respiratory infections.

2. Anti-myxovirus activity of polyoxotungstates

Before the examination for antiviral activity against myxoviruses it was necessary to make the cellular viral infection rate more efficient, since usually the cytopathic effect (CPE) of these viruses is too weak to allow the colorimetric method for the evaluation of the inhibitory activity of the compounds against the virus infection. At first the most appropriate tissue culture cells for each virus infection was selected. For influenza virus (FluV) and respiratory syncytial virus (RSV) MDCK (cells) and HEp-2 cells were used, as most workers in the field. These cells showed relatively clear CPE by viral infection and it was easy to detect the difference between the treated and mock treated cells by calorimetric MTT method. However, for the infections of paramyxovirus such as parainfluenza virus (PfluV) type 2 and 3, mumps virus (MPSV), measles virus (MLSV) and canine distemper virus (CDV) host cells needed to be selected. After several rounds of testing HMV cells (originating from human melanoma cells) for PfluV-2, PfluV-3, and MPSV, and B95a cells (human lymphoid cells) for MLSV were selected. Since both cells grow

* Corresponding author. Tel.: +81 24 521 7818; fax: +81 24 521 7924.
E-mail address: sshigeta@fmu.ac.jp (S. Shigeta).

0753-3322/$ - see front matter © 2006 Elsevier SAS. All rights reserved.
doi:10.1016/j.biopha.2006.03.009

in culture as suspended state, virus and cells were mixed well by shaking and the viral infection started. For an as yet unknown reason, a low speed centrifugation of the mixture facilitated virus infection rate and made the MTT method easy [1]. The low-speed centrifugation of virus and cells at the virus infection to cells was also employed for the monolayer cells such as MDCK, HEp-2 and Vero cells, and it also increased the viral infection efficiency. Sometimes a plaque reduction method was employed for the assay of RSV, MSLV and CDV, using HeLa cells for RSV and Vero cells for MLSV and CDV, respectively.

Four polyoxotungstates of different structural classes have been shown to have broad spectrum anti-myxovirus activities. They are HS-054 {$[Na_{16}Fe_4(H_2O)_2(P_2W_{15}O_{56})_2]nH_2O$, Wells–Dawson sandwich}, HS-058 {$[K_{10}Fe_4(H_2O)_2\ (PW_9O_{34})_2]nH_2O$, Keggin sandwich}, HS106 {$[(Me_3NH)_8Si_2W_{18}Nb_6O_{77}]nH_2O$, Dimerized Keggin}, and HS-158 [$K_{12}Nb_6P_2W_{12}O_{62}$, Wells–Dawson]. HS-106 is the same compound as JM2820. As shown in Table 1, all the polyoxotungstates exhibited potent inhibitory effects against FluV-A, RSV-A and B, MLSV and PfluV-2 without evident relationship to their particular cluster forms. Among these, HS-054 exhibited broad spectrum anti-myxovirus activity and its selectivity indices (SI) for FluV-A, RSV-A, MLSV and PfluV-2 were 333, 31, 167, and 111, respectively, which exceeded those of ribavirin for each virus.

In order to explore the antiviral mechanism of action of HS-058 against FluV-A and RSV, the compound was added to host cells (MDCK cells for FluV and HeLa cells for RSV) before, during and after virus infection. After the treatment the cells were extensively washed with maintenance medium (MS) and then changed to MS and maintained throughout the experiment. The EC_{50} for each virus was determined by the MTT method for FluV and the plaque reduction method for RSV. As shown in Table 2, when the compound was added to the virus-infected cultures at 1 hour before virus inoculation and maintained throughout the experiment, it was inhibitory against FluV at 0.7 μM and against RSV at 2.0 μM. When HS-058 was added to the culture at the adsorption stage (from 1 hour before to 1.5 hour after the virus inoculation) it was inhibitory against RSV but not against FluV. When the compound was added after adsorption (or penetration) and maintained throughout the experiment (from 1.5 to 120 hours after virus inoculation), it was inhibitory against both viruses at 4.1 and 5.8 μM, respectively (Table 2). This result makes evident HS-058 obviously inhibits the adsorption of RSV but not that of FluV. However, certain additional inhibitory effects of the compound against the infection process occurred after viral adsorption of both of the viruses, although the EC_{50} values for both in which assay the compound was added after virus adsorption were three to six times higher than in the assay in

Table 2
Time of addition and inhibitory effects of HS-058 on FluV-A and RSV replication

Time of addition of compound (hours) [a]	EC_{50} (μM) against	
	FluV-A	RSV-A
−1–120	0.7	2.0
−1–1.5	> 20	2.4
1.5–120	4.1	5.8
1.5–3	> 31	> 20

[a] Time of addition before or after virus inoculation. Cells were washed extensively after removal of compound.

Table 1
Inhibitory effects of four polyoxotungstates against several ortho- and paramyxoviruses

Virus and cell	EC_{50} and IC_{50} of polyoxotungstates(μM) [a]				
	HS-054	HS-058	HS-106	HS-158	Ribavirin
Antiviral activity					
FluV-A H3N2 (Ishikawa) [c]	0.6 (0.37–0.94)	1.4 (0.7–2.0)	2.8 (1.3–5.4)	2.8 (1.0–5.5)	3.7 (1.8–7.0)
FluV-B (Singapore)	35.5 (20–54)	13.9 (8.7–21.8)	45.7 (19.4–68)	36.5 (30–43)	5.1 (1.8–5.2)
RSV-A (Long)	2.8 (1.4–4.5)	5.6 (2.4–13.5)	9.8 (9.0–10.3)	14.2 (8.3–24.4)	4.7 (1.5–9.7)
RSV-B (SM-61-48)	7.8 [b]	3.1 [b]	4.5 [b]	2.7 [b]	1.6 [b]
MLSV (Edmonston)	0.3 (0.2–0.4)	0.8 (0.76–0.85)	> 35.5 (6.6–50)	1.4 (1.2–1.6)	5.2 (1.9–10)
MPSV (EXCH-3)	20.6 (15.5–20)	> 50	> 50	> 50	3.4 (3.4–7.1)
PfluV-2 (Greer)	1.8 (1.5–2.1)	0.43 (0.32–0.54)	7.8 (2.6–16.1)	24.1 (23.2–25)	8.9 (6.4–11.2)
PfluV-3 (C243)	28.0 (25–31)	> 50	> 50	> 50	17.2 (16.4–18.0)
Cytotoxicity					
MDCK	> 200	> 200	> 200	164	> 200
HEp-2	88	> 200	> 200	82.7	52.7
HMV-2	> 200	50	20.7	53.7	> 100
Vero	50	50	148	> 200	100

[a] Determined by MTT method. Values are averages of three or four independent experiments. Numbers in parentheses show the ranges of values.
[b] Data from one experiment.
[c] In parenthesis the names of the virus strains were shown.

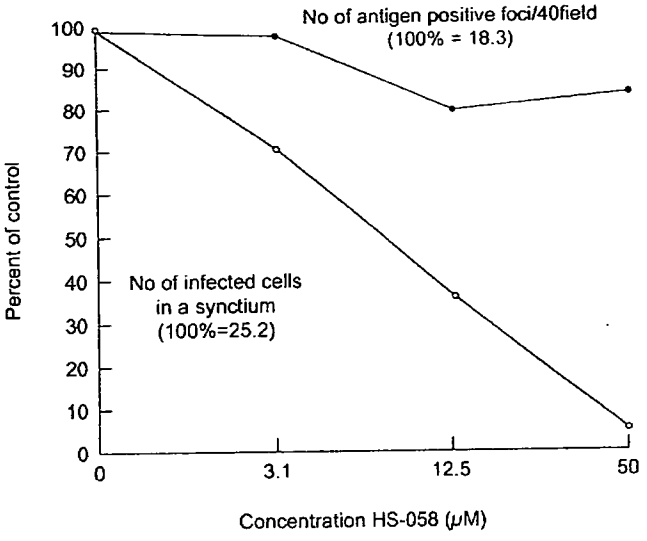

Fig. 1. Inhibitory effect of HS-058 on antigen synthesis and syncytium formation of RSV in HeLa cell monolayers.
HeLa cells grown on cover slips in culture plate wells were infected with 100 PFU/well of RSV. After virus adsorption to cells for 90 min at 37 C, infected cultures were treated with 3.1, 12.5 and 50 μM of HS-058 at 37 °C. At 48 hours after infection, cells on cover slips were fixed with acetone and stained with anti-RSV rabbit serum conjugated with fluorescein isothiocyanate. Cells were observed under a fluorescent microscope, and the number of antigen positive foci in 40 microscopic fields (•) and the number of infected cells in one syncytium (○) [average of 10 syncytia] were counted.

Table 3
Inhibition of FluV and RSV infection by HS-058

Infection process	FluV-A	RSV-A
Adsorption to cell membrane	No	Yes
Fusion of virus envelope and cell membrane	Yes	Unclear
RNA and protein synthesis	Probably no	Probably no
Fusion between infected and uninfected cells	Unclear	Yes

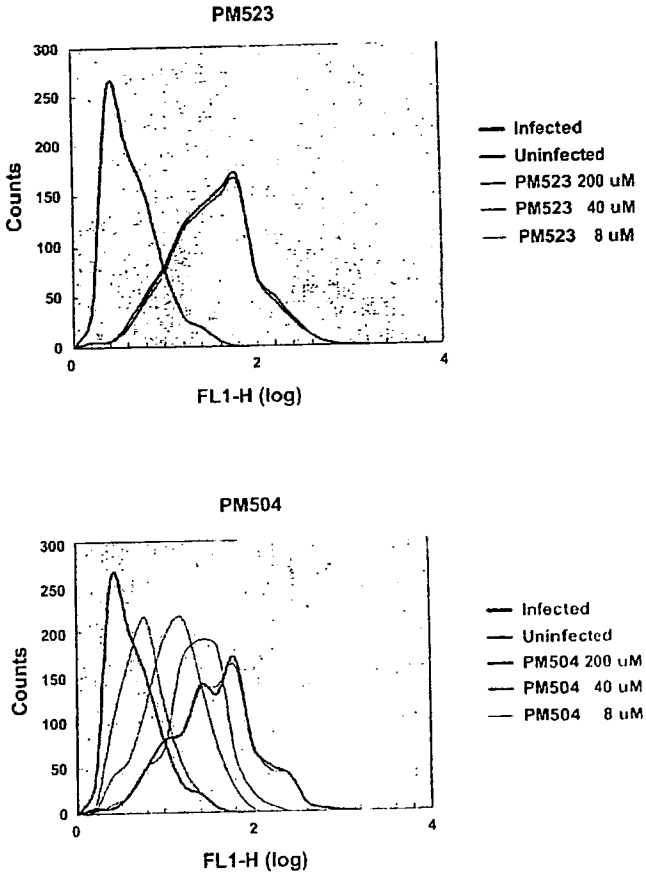

Fig. 2. Fax scan (FACS) analysis of FluV A binding to MDCK cells and its inhibition by PM-523 and PM-504.
MDCK cells were mixed with FluV A at a moi of 1 and incubated at 37 °C for 1.5 hour. During the incubation, 8–200 μM of compounds were combined with the virus-cell mixture. After incubation, binding of FluV to cells was examined by mouse serum and FITC-conjugated goat anti-mouse IgG antibody. Abscissa indicates intensity of fluorescence and ordinate indicates number of cells. Bold lines in the right peaks are populations of infected cells without compound and the lines in the left peaks are those of uninfected cells.

which the compound had been added at all points of the progress of the viral infections. In fact, in another experiment, HS-058 inhibited hemolysis of chicken erythrocytes (fusion of the virus envelope and the cellular membrane) by FluV at 58 μM (data not shown) and syncytium formation (fusion of the virus infected cells with uninfected cells) of RSV at 8.5 μM (Fig. 1 and Table 3) [2].

3. Mechanism of anti-FluV activity of polyoxotungstates

As described above, polyoxotungstate did not inhibit the binding of FluV to the cellular membrane and probably the antiviral effect occurs at a later step of virus replication. We examined the other polyoxotungstates which contain titanium as a heterometal ion. These are PM-504 [$K_9H_6(Ge_2Ti_6W_{18}O_{77})_{16}H_2O$, Double Keggin] and PM-523 [$\{(iPrNH_3)_6H[PTi_2W_{10}O_{38}(O_2)_2]H_2O$, Keggin}. The EC_{50} values of PM-504 and PM-523 against FluV A were 1.3 and 2.4 μM and the SIs were more than 300 and 167, respectively. We examined fax scan (FACS) analysis of virus bound MDCK cells and inhibition by both compounds, and found that PM-504 inhibited the binding of FluV to the cells and PM-523 did not (Fig. 2, and see the legend for the figure for the experimental procedure).

The penetration of enveloped viruses is widely reported to start by the fusion of the viral envelope with the cellular membrane. The fusion of the FluV envelope with the cellular membrane occurs under acidic conditions in the endosome. When the virion envelope is labeled compactly with fluorescent molecules (i.e., octadecyl rhodamine B chloride), the fluorescence is quenched and cannot be detected by a fluorometer. After contact between the viral envelope and cell membrane and membrane fusion has taken place, the viral protein molecules that were labeled by fluorescence move to the cell membrane. As a result the density of the molecule decreases and fluorescence is recovered (dequenched) (Fig. 3). In order to analyze the inhibition of the fusion of the virus envelope with the cell membrane, the fluorescence dequenching test was performed using rhodamine-labeled virus particles and MDCK cells. During the interaction of fluorescein-labeled virus and the cell membrane, the

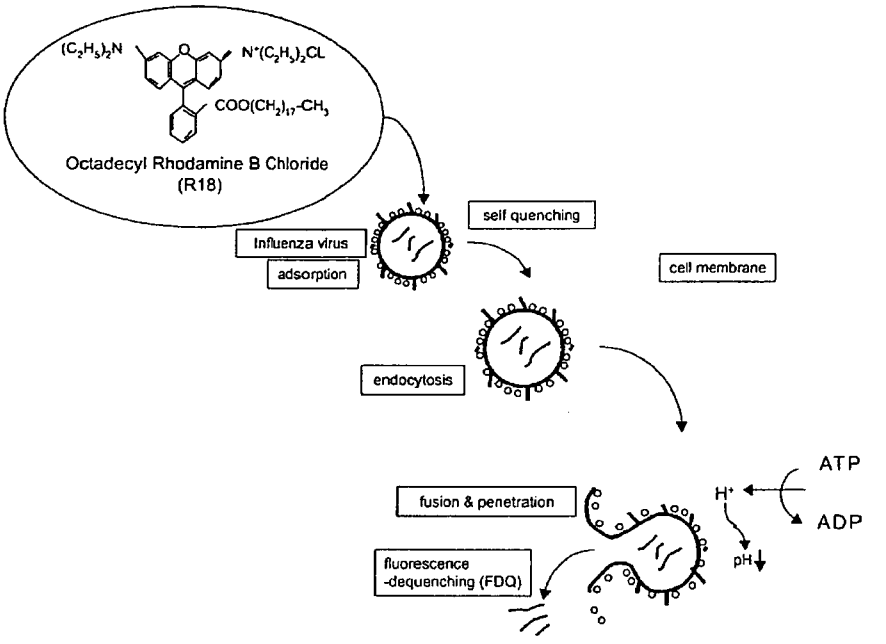

Fig. 3. Fluorescence dequenching test.
FluV envelope proteins are labeled with rhodamine chloride (R-18). When the density of fluorescent protein molecule is too compact, the fluorescence is quenched and cannot be detected. After endocytosis of the virion, when fusion of viral envelope to cell membrane is completed, fluorescent molecules move to cell membrane, are dispersed in the membrane, and the self quenched fluorescence is recovered. The degree of the fluorescence dequenching (FDQ) is measured by a fluorometer.

flurescence increased gradually as a factor of the contact period. When PM-523 (a titanium containing polyoxotungstate) was added during the contact between the virus and the cell membrane, the dequenching of the fluorescence by the fused membrane was remarkably reduced compared with the untreated membrane in contact with the virus for the same period (Fig. 4). The inhibition was observed for the fusion of two different subtypes of FluV A (N3H2/Ishikawa and H1N1/PR8), but not for those of FluV B or Sendai virus (a PfluV type 1) (data not shown). Thus the inhibitory activity of PM-523 was shown to be specific to FluV A [3].

4. PM-523 resistant FluV A strains

We selected PM-523 resistant FluV A strains after several passages of FluV A H3N2/Ishikawa in MDCK cells in the presence of an effective dose of PM-523. R-1 to R-c were resistant to PM 523, and their EC_{50}s were 10 times higher than that of the parental strain. When amino acid substitution in the HA1 protein between the parent and mutant strains were analyzed, lysin189 and isoleucin202 were substituted with asparagine and threonine, respectively (Table 4). Lysine189 and isoleusine202 locate at the head position of HA1 and this position is at the interface of the HA1 trimer. PM-523 probably inhibits the opening of the head when the conformational change of the HA molecule occurs (Fig. 5) [4]. Thus the mechanism of the anti-FluV A activity of PM-523 is shown to be inhibition of membrane fusion; however, the mechanism is dependent on the nature and structure of the particular POM, because another POM, PM-504, inhibited the binding of FluV A to MDCK cells.

5. Synergistic anti-FluV A activities of PM-523 and ribavirin in vitro and in vivo

Because the antiviral activity of PM-523 was revealed to be inhibition of the fusion of the viral envelope with the cell membrane, PM-523 may have synergistic antiviral activity against FluV replication when used in combination with compounds with a different antiviral target. Ribavirin is a well-known antiviral compound which inhibits inocine monophosphate dehydrogenase activity in cells and decrease the guanosine monophosphate pool which suppresses viral RVA synthesis.

We examined anti-FluV A activity with several different ratio combination of PM-523 and ribavirin in vitro and compared this with the individual respective compounds in terms of the effective dose by several parameters of inhibition. MDCK cells were infected with FluV (H1N1/PR8). Two fold serial dilutions from 0.8 mM stock dilutions of PM-523 and ribavirin were combined in a checkerboard cross grid. The median effective dose and other doses (EC_{50}, EC_{70}, EC_{90} etc.). were determined by the MTT method for PM-523 alone, ribavirin alone, and several different ratio combinations of the compounds. The predicted percent inhibition values were derived from a theoretical dose–response curve generated from the individual dose–response data for PM-523 and riba-

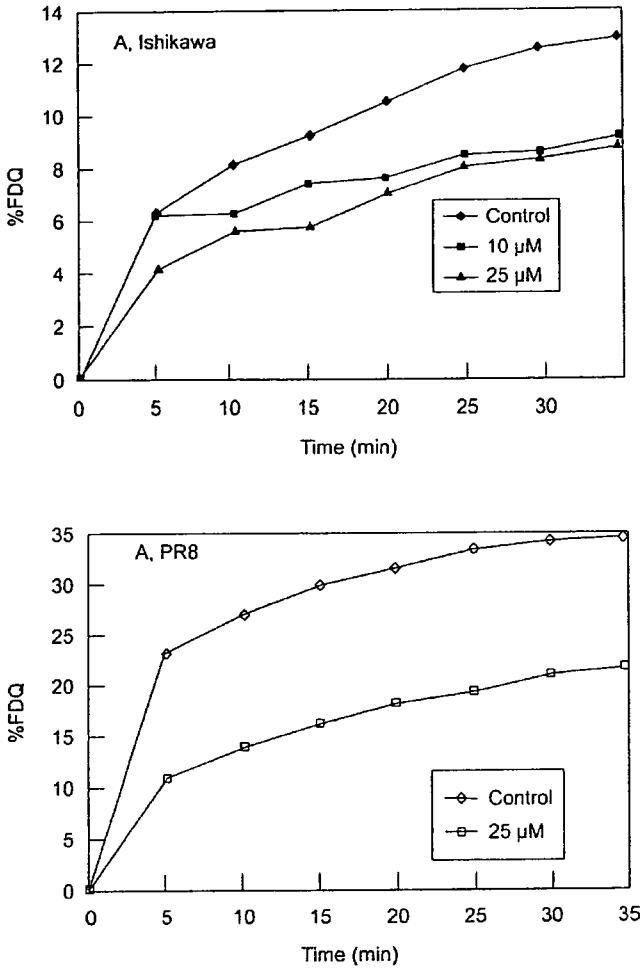

Fig. 4. Effect of PM-523 on dequenching of rhodamine B (R-18) on FluV envelope by fusion with cellular membrane.
The increase in fluorescence was expressed in percentage of FDQ. FluV/A/Ishikawa/H3N2 and PR8/H1N1 were used. Control (♦—♦), 10 μM (●—●), 25 μM (■—■) of compounds were added.

Table 4
PM 523 resistant strains and amino acid changes in HA of the resistant strains

	EC_{50} (μM) [a]		
Virus stock	MTT	Plaque reduction	Amino acid substitution
Parent [b]	8.7 ± 1.2	6.6 ± 0.8	
R-1 [c]	71.4 ± 6.8	74.5 ± 10.2	Lys189Asn, Ile202Thr
R-2 [c]	67.8 ± 6.5	73.6 ± 10.8	Ile202Thr
R-4 [c]	79.0 ± 10.2	88.1 ± 9.9	Ile202Thr
R-b [d]	63.0 ± 7.0	66.7 ± 6.2	Lys189Asn
R-c [d]	80.3 ± 6.8	78.9 ± 9.4	Lys189Asn, Ile202Val

[a] Values are averages of three independent experiments.
[b] Ishikawa/AH3N2/(plaque purified) strain.
[c] Progenies of the parent strain.
[d] Progenies of a wild Ishikawa strain.

virin. The combination index (CI) was calculated from the equation; CI = d1/D1 + d2/D2 + α(d1xd2/D1xD2), where d1and d2 indicate the fractional dose of a combination of compound 1 and 2, respectively, which are required for a median effect or a 70% inhibitory effect. D1 and D2 are the doses of the compound 1 and 2, respectively, which are required to produce the same median effect or 70% inhibitory effect when these compounds were used alone. In the case of PM-523 and ribavirin, α is 1 because both compounds were mutually nonexclusive drugs in terms of the mechanism of action. When the CI is <1, synergism is indicated. When the CI is 1, the

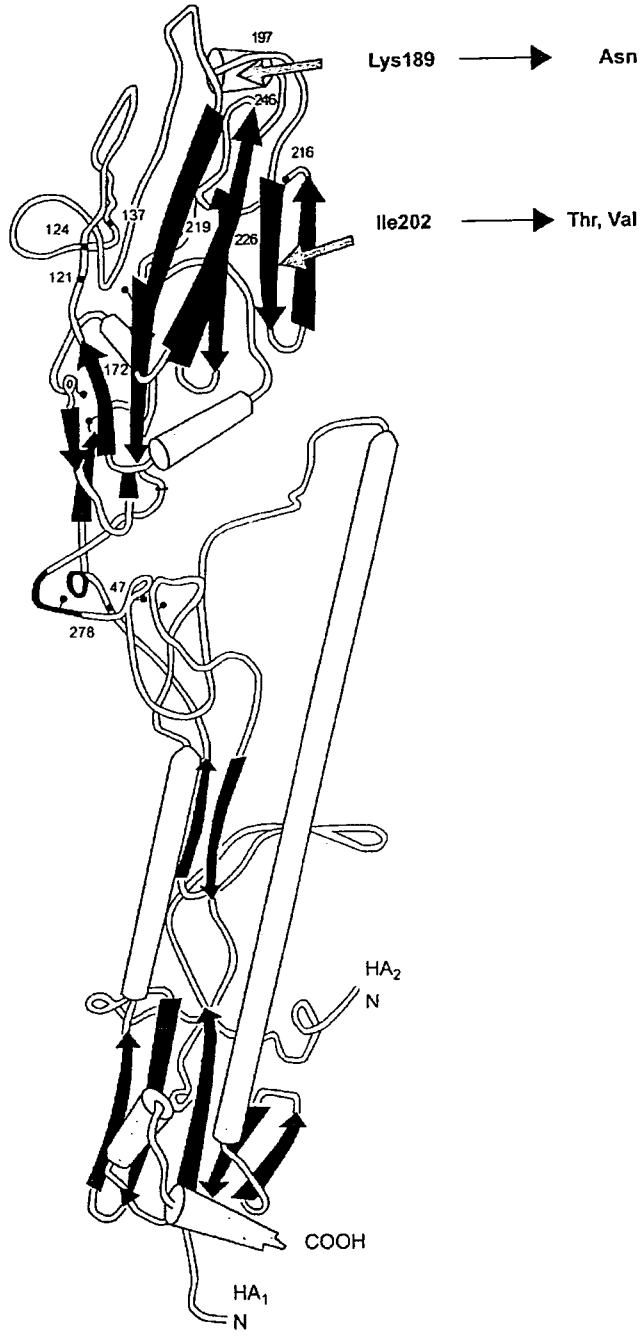

Fig. 5. 3-D structure of FluVA-HA peptide.
Both Lys189 and Ill202 locate at the head position of HA1. Arrows indicate the position.